Harmful Algae 151 (2026) 103026

Contents lists available at ScienceDirect

Harmful Algae

journal homepage: www.elsevier.com/locate/hal

Morphological, molecular and toxinological characterization of potentially toxigenic microalgal strains from the western Black Sea

Fuat Dursun [a], Nina Dzhembekova [b], Bernd Krock [c], Jan Tebben [c], Urban Tillmann [c,*]

[a] Institute of Marine Sciences and Management, University of Istanbul, Fatih, İstanbul 34134, Türkiye
[b] Institute of Oceanology "Fridtjof Nansen"–Bulgarian Academy of Sciences, Varna 9000, Bulgaria
[c] Alfred Wegener Institut-Helmholtz Zentrum für Polar- und Meeresforschung, Ökologische Chemie, Bremerhaven 27570, Germany

ARTICLE INFO

Keywords:
Dinoflagellates
Phylogeny
Phycotoxin
Liquid chromatography-tandem mass spectrometry
Characteristic spirolides

ABSTRACT

Harmful algal blooms (HAB) of various toxic microalgae negatively affect the Black Sea but there is limited data on the sources of phycotoxins in this area. During the PHYCOB cruise in September 2021, two strains of one diatom and thirty strains of ten dinoflagellate species of potentially toxigenic plankton were characterized in terms of morphology, phylogeny, toxin profiles, and toxin cell quotas. Twenty strains of potentially yessotoxins (YTXs) producing dinoflagellate species were investigated. All six strains of *Protoceratium reticulatum* contained yessotoxin (YTX), with cell quotas between 1.9 and 5.4 pg cell^{-1}. Additionally, several YTX variants were detected in minor amounts in nine of twelve strains of *Lingulaulax polyedra*, whereas no YTXs were detected in two strains of other gonyaulacoids (*Gonyaulax* sp. and *Sourniaea diacantha*). All strains of *Alexandrium* spp. (four strains of *A. tamutum*, one strain each of *A. andersonii, A. ostenfeldii*, and *A. pseudogonyaulax*) were analyzed for all toxins known to be produced by the genus. None of the strains contained detectable levels of paralytic shellfish toxins (PSTs) or gymnodimines. *A. pseudogonyaulax* produced goniodomine A (GDA) and GDA-seco acid at cellular levels of 14.0 and 0.33 pg cell^{-1}, respectively. Moreover, four previously unreported spirolide analogues (SPX) were detected in the *A. ostenfeldii* strain, with cell quotas between 1.0 and 1.6 pg cell^{-1}. All strains of potentially ichthyotoxic species (*Karlodinium* sp., *Polykrikos hartmanii*) did not show extracellular lytic activity. In conclusion, these findings improve our understanding of the potential sources, diversity and dynamics of phycotoxins in the Black Sea.

1. Introduction

In recent years, harmful algal blooms (HABs) have occurred with increasing frequency globally (Glibert et al., 2005; Hallegraeff, 2010) with negative impacts primarily resulting from the production of potent toxins. Such toxigenic species are associated with various phycotoxins that may cause fish kills or pose a serious risk to human health by accumulation throughout the food chain, causing different types of poisoning syndromes, including paralytic shellfish poisoning (PSP), diarrhetic shellfish poisoning (DSP), neurotoxic shellfish poisoning (NSP), amnesic shellfish poisoning (ASP), and azaspiracid shellfish poisoning (AZP) (Farabegoli et al., 2018). Additionally, poisoning syndromes and their causative species are region-specific (Hallegraeff et al., 2021).

The Black Sea is an isolated marine basin characterized by low salinity due to intense freshwater influx, permanent vertical stratification, and an anoxic layer below 150–200 m depth (Zaitsev and Mamaev, 1997). Plankton blooms have been considered one of the key issues affecting the health of the Black Sea ecosystem (Moncheva et al., 1995; Velikova et al., 1999; Nesterova et al., 2008). Furthermore, the introduction of new toxic microalgal species via the Bosporus (İstanbul Boğazı), which could acclimatize and form large blooms, has been suggested as a potential risk (Bodeanu and Roban, 1975). Microplankton biodiversity in the Black Sea has been extensively studied in the second half of the 20th century, primarily using traditional light microscopy methods (Nesterova et al., 2008; Moncheva and Parr, 2015). With this approach, over 1600 microalgal species were identified (Moncheva and Parr, 2015). About 49 of these species are classified as toxigenic or harmful in other aspects (Ryabushko, 2003a), but their presence in almost all cases in fact is insufficiently documented. The lack of advanced investigations for species identification and characterization has been recognized as a critical knowledge gap in the Black Sea basin,

* Corresponding author.
E-mail address: urban.tillmann@awi.de (U. Tillmann).

https://doi.org/10.1016/j.hal.2025.103026
Received 19 May 2025; Received in revised form 23 September 2025; Accepted 11 November 2025
Available online 12 November 2025

particularly crucial for potentially toxic plankton species (Moncheva et al., 2019). Additionally, the toxigenic capacity of local populations of harmful species in the Black Sea and their biogeography remain under-researched (Moncheva et al., 2019). In fact, there are only two reports on strain-based identification of toxin production potential of local species, including domoic acid production by a strain of *Pseudo-nitzschia calliantha* from Sevastopol Bay (Besiktepe et al., 2008) and okadaic acid and DTX-1 production by cultured material of *Prorocentrum lima* from the Russian Caucasian Black Sea Coast (Morton et al., 2009).

In the Black Sea, a wide range of phycotoxins, including paralytic shellfish toxins, diarrhetic shellfish toxins, pectenotoxins, yessotoxins, and domoic acid, have been detected in wild and aquaculture mussels, as well as in plankton samples from the Bulgarian and Russian coasts (Vershinin and Kamnev, 2001; Vershinin et al., 2005, 2006; Morton et al., 2007, 2009; Peneva et al., 2011; Kalinova et al., 2015; Krumova–Valcheva and Kalinova, 2017; Peteva et al., 2019, 2020; Dzhembekova et al., 2022). In the Bulgarian part of the Black Sea, long-term data list the presence of 28 potentially toxic species (Dzhembekova and Moncheva, 2014). Many of these species are common in plankton communities in Bulgarian waters (*Alexandrium* spp., *Gonyaulax* spp., *Lingulaulax polyedra, Prorocentrum* spp., *Pseudo-nitzschia* spp.), and some of them are typical "bloom-forming" taxa (*Prorocentrum* spp., *Pseudo-nitzschia* spp.). The distribution of HAB species along the Romanian littoral is similar, with 11 potentially toxic species recorded. These include the diatoms *Pseudo-nitzschia delicatissima, P. pungens*, and *P. seriata* (potential producers of domoic acid) and the dinoflagellates *Dinophysis acuminata, D. acuta, D. caudata, D. sacculus* (producers of dinophysistoxins, okadaic acid, and pectenotoxins), *Protoceratium reticulatum* (yessotoxin producer), and *Prorocentrum cordatum*. The recent application of molecular methods additionally indicate presence of previously overlooked potentially toxic species, such as *Pseudo-nitzschia calliantha, Karenia bicuneiformis, Karlodinium veneficum*, and *Pfiesteria piscicida* (Dzhembekova et al., 2017a, 2017b).

In most cases, no detailed investigations have been conducted to determine the sources of phycotoxins in the western Black Sea, and still little is known about the characteristics of toxigenic microalgal species in the region. In this context, the PHYCOB project was developed to expand knowledge of HAB threats in the Black Sea. The specific aim of the present study was to isolate potentially toxigenic taxa from the western Black Sea during the PHYCOB cruise in 2021 and to characterize the strains in terms of morphology, phylogeny, toxin profiles, and toxin cell quotas. From the same project and cruise, detailed data on the distribution and abundance of potentially toxic microalgae in the field samples of the 2021 survey were also analyzed together with the determination of phycotoxin levels in size-fractionated field samples, these results are published and available in a companion paper (Dzhembekova et al., 2025). This combined approach enhances the knowledge of which plankton species are responsible for, or contribute to, the phycotoxins found in Black Sea field samples.

2. Material and methods

2.1. Sample collection and isolation of strains

Samples were collected during the PHYCOB survey on board the R/V TÜBİTAK MARMARA from 11th September to 17th September 2021 covering the western Black Sea (Romanian and Bulgarian waters) (Fig. 1). For a detailed description of the sampling protocol see Dzhembekova et al. (2025).

Cell isolations were performed using net tow samples and a stereo microscope by using microcapillary to isolate single cells into individual wells of a 96-well plate pre-filled with filtered seawater (FSW) from the

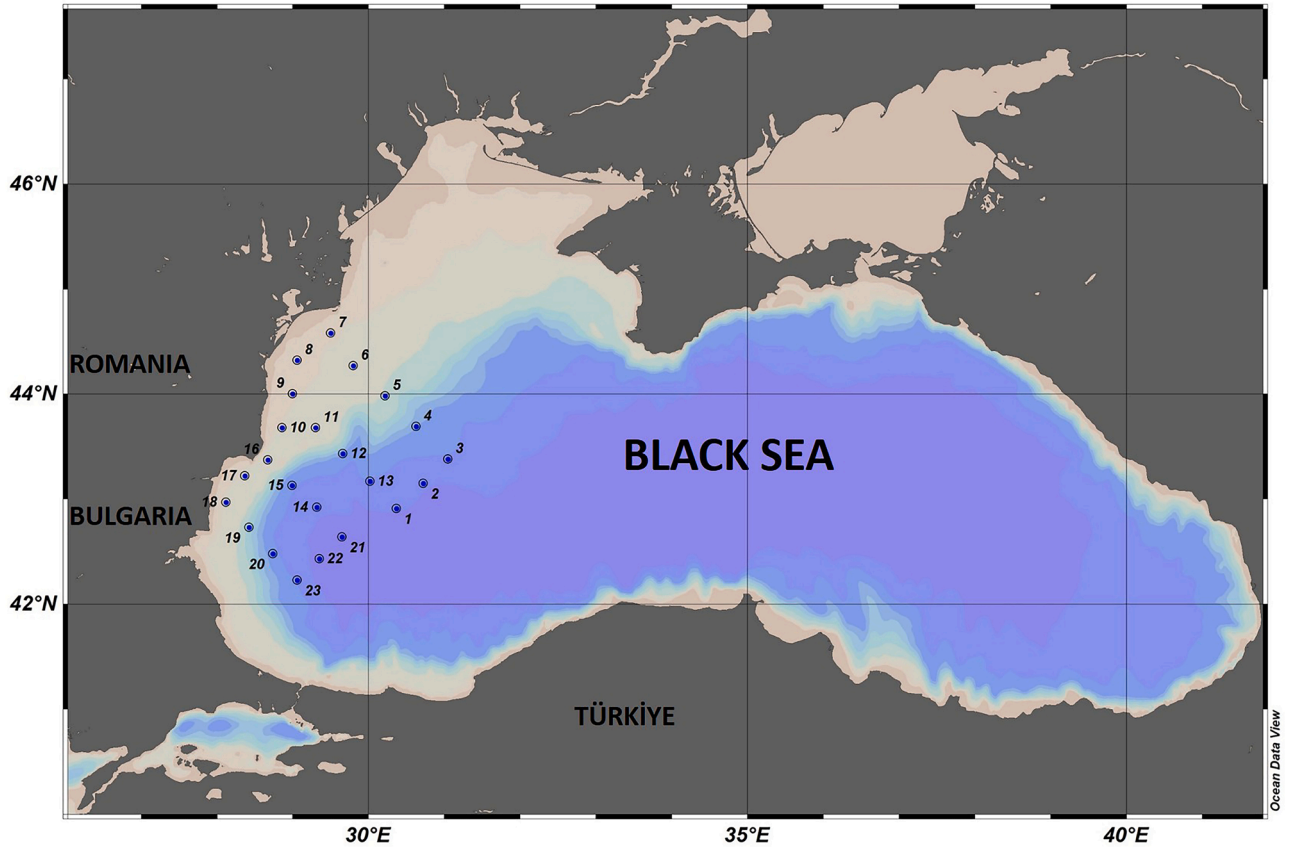

Fig. 1. Map of the study area and sampling stations on the PHYCOB expedition in September 2021. The map was created using Ocean Data View (Schlitzer, Reiner, Ocean Data View, https://odv.aw.de, 2023).

sampling site, with the surface water salinity at the stations where cells were isolated ranging between 18 and 19. Isolation plates from the cruise were kept in a temperature-controlled incubator (Model MIR 252, Sanyo Electric Biomedical Co., Osaka, Japan) at 20 °C and 16:8 h light: dark photocycle at a photon flux density of approximately 50 μmol m^{-2} s^{-1} and were regularly inspected for growth. Growing strains were transferred to 70 mL plastic culture flasks and stock cultures were routinely grown at the same conditions described above. Among all strains obtained from the cruise, 32 strains were identified as potentially toxigenic species (Table 1). All strains were grown using K-medium (Keller et al., 1987) prepared with sterile filtered (0.1 μm VacuCap filters, Pall Life Sciences, Dreieich, Germany) North Sea water (diluted from salinity ~32–33 to 20 with deionized water). The original K-recipe was slightly modified by replacing organic phosphorus with inorganic phosphate. Also, silicate was added to the medium for *Pseudo-nitzschia* strains only. The pH of the culture medium was adjusted to 8.0 by adding 1 M hydrochloric acid.

2.2. Morphological characterization of strains

Light microscopy (LM) observations of living or fixed cells of the collected strains were carried out using epifluorescence and high resolution (up to 1000 × magnification) Axiovert 200 M and Axioskop 2 (both Zeiss), both coupled with a digital camera (MRc5, Zeiss) and a video camera (Gryphax, Jenoptik). Cell length and width were measured at 400 × or 1000 × magnifications using Axiovision software (Zeiss), and sizes are reported as mean values and the ranges (minimum (mean) maximum μm). LM examination of thecal plates was performed on fixed cells (neutral Lugol) stained with Solophenyl Flavine 7GFE500, a fluorescent dye specific to cellulose (Chomérat, 2016), which were examined with epifluorescence filter set 09 (Zeiss; BP 450–490; FT 510; LP 515).

2.3. DNA extraction and phylogenetic analyses

For DNA extraction, strains were grown under the standard culture conditions described above. 50 mL of a healthy and growing culture (based on stereomicroscopic inspection of the live culture) were harvested by centrifugation (Eppendorf 5810R, Eppendorf, Hamburg, Germany; 3220 × *g*, 10 min). Each pellet was transferred to a microtube, centrifuged again (Eppendorf 5415; 16,000 × *g*, 5 min), resuspended in 0.5 mL SL1 lysis buffer (provided by the DNA extraction kit), and stored at −20 °C until DNA extraction.

DNA was extracted using the NucleoSpin Soil DNA extraction kit (Macherey and Nagel, Düren, Germany). The DNA extraction followed the manufacturer's instructions, with slight variation. Instead of vortexing, the bead tubes were shaken for 45 s and another 30 s at a speed of 4.0 m s^{-1} in a cell disrupter (FastPrep FP120, Thermo-Savant, Illkirch, France). For DNA elution, 2 × 50 μL of the provided elution buffer were used (for a final elution volume of 100 μL) to maximize the overall DNA yield. DNA was stored at −20 °C until further processing.

To determine the ITS and LSU rDNA sequences, the following forward and reverse primers were used: ITSA and ITSB (Sato et al., 2011), and D1R and D2C (Scholin et al., 1994) for dinoflagellates; ITS1 and ITS4 (White et al., 1990), and D1R (Scholin et al., 1994) and D3B (Nunn et al., 1996) for diatoms (*Pseudo-nitzschia*). PCR amplification of genomic DNA was performed in 20 μL reaction volume using AccuPower® HotStart PCR PreMix (Bioneer Corporation, Republic of Korea). The reaction mix contained 0.5 μL of each primer (0.25 μM) and approximately 15 ng of DNA. The PCR amplification protocol included an initial denaturation step at 94 °C for 5 min, followed by 30 cycles of 30 s at 94 °C, 1 min at 55 °C, and 1 min at 72 °C, with a final extension at 72 °C for 5 min. PCR products were purified and sequenced in both directions at Macrogen Europe. The sequences were manually edited using MEGA version X (Kumar et al., 2018) and are available in the GenBank database (Clark et al., 2016) (Table S1).

The obtained sequences were analyzed using the NCBI BLAST online

Table 1
Compilation of potentially toxic microalgal strain obtained during the PHYCOB 2021 cruise.

Species	Strain	Station nr	Coordinates DD Latitude, Longitude
Pseudo-nitzschia calliantha	BS 3-F11	19	42.73, 28.42
	BS 4-H4	19	42.73, 28.42
Alexandrium andersonii	BS 5-E11	11	43.69, 29.30
Alexandrium ostenfeldii	BS 5-D3	15	43.13, 28.99
Alexandrium pseudogonyaulax	BS 6-D1	19	42.73, 28.42
Alexandrium tamutum	BS 4-A1	3	43.38, 31.05
	BS 5-C12	10	43.68, 28.85
	BS 3-D6	10	43.68, 28.85
	BS 5-C7	15	43.13, 28.99
Gonyaulax sp.	BS 5-E4	19	42.73, 28.42
Sourniaea diacantha	BS 6-D7	20	42.48, 28.74
Protoceratium reticulatum	BS 6-E4	2	43.15, 30.72
	BS 6-F10	5	43.98, 30.22
	BS 4-F3	5	43.98, 30.22
	BS 4-B11	11	43.69, 29.30
	BS 6-H12	19	42.73, 28.42
	BS 4-F11	20	42.48, 28.74
Lingulaulax polyedra	BS 5-C11	3	43.38, 31.05
	BS 4-F12	5	43.98, 30.22
	BS 5-D2	5	43.98, 30.22
	BS 3-D5	10	43.68, 28.85
	BS 4-B8	10	43.68, 28.85
	BS 4-G3	10	43.68, 28.85
	BS 5-C9	11	43.69, 29.30
	BS 6-E1	13	43.17, 30.02
	BS 4-G4	15	43.13, 28.99
	BS 3-E1	16	43.37, 28.67
	BS 5-E8	19	42.73, 28.42
	BS 3-E6	20	42.48, 28.74
Karlodinium sp.	BS 3-F8B	2	43.15, 30.72
	BS 6-E10	15	43.13, 28.99
Polykrikos hartmannii	BS 7-E9	9	44.00, 28.99

tool (https://blast.ncbi.nlm.nih.gov/Blast.cgi) to identify sequences with the highest similarity.

Separate datasets were compiled using sequences from the studied Black Sea strains and sequences obtained from the GenBank database (Clark et al., 2016) (Tables S2–S5). The sequence alignments were performed using ClustalW (Thompson et al., 1994) with default settings implemented in MEGA version X (Kumar et al., 2018), except for the *Alexandrium* phylogenetic analyses, where the MAFFT version 7 (Katoh et al., 2019) online program (http://mafft.cbrc.jp/alignment/server/) was used with default settings.

The phylogenetic relationships were determined using the maximum likelihood (ML) method in MEGA X (Kumar et al., 2018) and the bayesian inference (BI) method in MrBayes v.3.2 (Ronquist and Huelsenbeck, 2003). For BI, four Markov chain Monte Carlo (MCMC) chains were run for 1,000,000 generations, sampling every 100 generations. The first 25 % of burn-in trees were discarded. The phylogenetic trees were represented using the ML results, with bootstrap values from the ML method (1000 replicates) and posterior probabilities from the BI method. All sites were used for analyses. Details regarding the sequences used, the number of positions in the final datasets, and the models applied are provided in the supplementary material (Tables S2–S5).

Evolutionary divergence among the strains of *Sourniaea diacantha* and species of the Kareniaceae family was estimated using the Pairwise Distance method with default settings in MEGA X (Kumar et al., 2018) (Tables S6–S9).

2.4. Toxin screening

For toxin analysis, strains were grown as batch cultures under the standard culture conditions described above. Cells were harvested at late exponential/early stationary phase, and for each harvest, cell density was determined by settling Lugol's fixed samples and counting >400 cells under an inverted microscope in order to calculate toxin cell quota. 50 mL subsamples of strains were harvested by centrifugation at 3220 × *g* for 10 min. After decanting the supernatant, the cell pellets were resuspended in the residual medium, transferred to a microtube, centrifuged again (16,000 × *g*, 5 min), and stored frozen (−20 °C) until further processing. For a number of selected strains, growth and harvest procedures were repeated several times to yield high biomass for an increased sensitivity of the toxin detection method.

Cell pellets were transferred to 2 mL microcentrifuge tubes containing 0.9 g lysing matrix D (Thermo Savant, Illkirch, France). Subsequently, the pellets were suspended in 500 μL 0.3 M acetic acid for PSTs and in 500 μL methanol for liphophilic toxins, and homogenized by reciprocal shaking at maximum speed (6.5 m s^{-1}) for 45 s with FP120 FastPrep instrument (Bio101, Thermo Savant). After homogenization, the samples were centrifuged (16,000 × *g*, 15 min, 4 °C) again and the supernatants were transferred to a spin-filter (pore-size 0.45 μm, Millipore Ultrafree, Eschborn, Germany) and centrifuged for 30 s at 3220 × *g*. Filtrates were transferred into HPLC vials (Agilent Technologies, Waldbronn, Germany) and stored at −20 °C.

For domoic acid (DA) analysis, 50 mL sub-samples from culture flasks were taken and filtrated through GF/C filter (25 mm diameter, 1.2 μm, Sigma-Aldrich, Taufkirchen, Germany) with a gentle vacuum. Cells with the filter were transferred to 2 mL microcentrifuge tubes containing 0.9 g lysing matrix D (Thermo-Savant, Illkich, France). 1 mL of a 1:1 mixture of 50 % methanol and 0.03 M acetic acid was added to the tube and homogenized by reciprocal shaking at maximum speed (6.5 m s^{-1}) for 45 s with FastPrep instrument (Thermo Savant). After homogenization, the samples were centrifuged (16,000 × *g*, 5 min, 4 °C) and the supernatant was transferred to a spin-filter with a pore size of 0.45 μm Nylon membrane (Millipore, Echborn, Germany) and centrifuged for 30 s at 3220 × *g*. Filtrates were transferred into HPLC vials and stored at −20 °C until analysis (Weber et al., 2021).

2.4.1. PST analyses

The aqueous extracts were analyzed for PSP toxins by reverse-phase ion-pair liquid chromatography (LC) coupled to post-column derivatization with fluorescence detection (PCOX) following minor modifications of previously published methods (Diener et al., 2006; Krock et al., 2007). For details see the supplementary material - analytical methods.

2.4.2. Analysis of lipophilic toxins

Ultraperformance liquid chromatography (UPLC®) coupled with tandem quadrupole mass spectrometry (LC-MS/MS) analysis for multiple lipophilic toxins (including DA) was performed. The UPLC system included a column oven, an autosampler and a binary pump (AQUITY I UPLC Class, Waters, Eschborn, Germany). For details see the supplementary material - analytical methods.

2.4.2.1. YTX analyses. In addition to the multiple lipophilic toxin analysis, variants of YTX (selected transitions (precursor ion > fragment ion) were given in Table S10) were scanned specifically by the SRM in the negative ion mode on a LC-MS/MS system consisting of a LC chromatograph (LC1100, Agilent) and an API 4000-QTrap tandem mass spectrometer (Sciex, Darmstadt, Germany).

2.4.2.2. Cycloimine analyses. The cycloimine measurements were performed based on the method which was described before by Martens et al. (2017). In brief, SPX were calibrated against an external calibration curve of 13-desmethyl-spirolide C (SPX-1; certified reference material (CRM); NRC, Halifax, NS, Canada) and expressed as SPX-1 equivalents. For the calibration curve, the following concentrations of SPX-1 were used: 10 pg μL^{-1}, 50 pg μL^{-1}, 100 pg μL^{-1}, and 1000 pg μL^{-1}. Likewise, gymnodimines (GYM) were calibrated against an external calibration curve of GYM A (CRM; NRC) and expressed as GYM A equivalent. 12-Methyl-gymnodimine A was purchased from Biomol GmbH (Hamburg, Germany) and used for compound identification. For quantification of GYM, the following concentrations of a standard solution of GYM A were used: 10 pg μL^{-1}, 50 pg μL^{-1}, 500 pg μL^{-1}, and 1000 pg μL^{-1}. For cycloimine screening, transitions of the all known GYM and SPX were included in the method and given in Table S11. The accurate masses of four novel SPX were determined by Ultra-High-Performance Liquid Chromatography (UHPLC) coupled to a high-resolution mass spectrometer (Q-Exactive Plus, both Thermo Fisher Scientific, Schwerte, Germany). For details see the supplementary material - analytical methods.

2.4.2.3. Karlotoxin (KmTx) analyses. KmTx-2 standard solution (23 ng μL^{-1}) was run in SRM method with typical KmTx fragments in the positive ion mode, to determine the possible presence of KmTx-related compounds. 1367 → 937 mass transition was run for karlotoxin screening in the LC-MS analysis. Experiments were performed based on the method which was described before by Krock et al. (2017).

2.4.3. Extracellular lytic activity

Extracellular lytic activity of both strains of *Karlodinium* sp. and *Polykrikos hartmannii* was estimated using a bioassay with the cryptophyte *Cryptomonas* (strain KAC 30 from Kalmar culture collection) as target species grown at the standard conditions as outlined above. In brief, intact *C. salina* cells were microscopically counted after 24 h treatment with supernatant of the three strains compared to cell numbers of a control (treated with culture medium). A 30 mL subsample of *Karlodinium* sp. and *Polykrikos hartmannii* cultures in early stationary phase was centrifuged for 10 min at 3220 × *g*. The supernatant was divided into triplicate glass vials (4 mL each). To each vial, 0.1 mL of *Cryptomonas salina* (adjusted to 1 × 10^4 cells mL^{-1}) was added. Samples and controls (culture medium only) were incubated in the dark at 20 °C for 24 h. After incubation, 0.5 mL subsamples were fixed with Lugol's iodine (2 % final concentration), and intact *C. salina* cells were counted

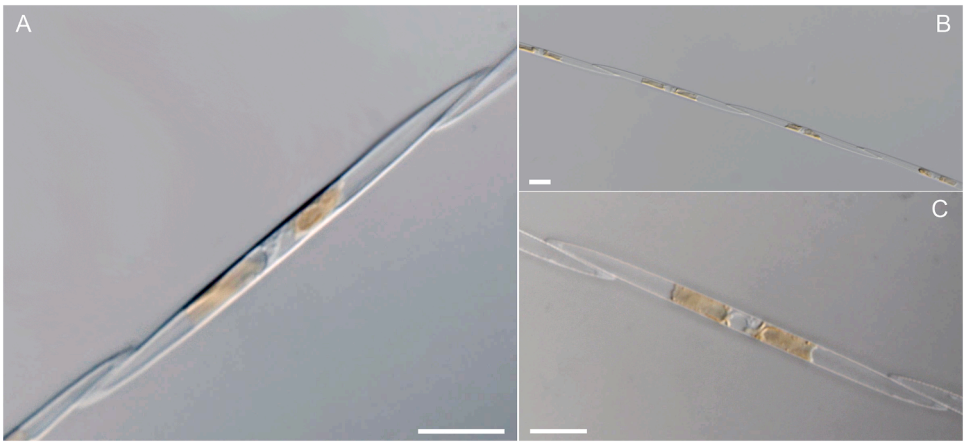

Fig. 2. Light microscopy images of living cells of *Pseudo-nitzschia calliantha* strain BS 3-F11 (A) and strain BS 4-H4 (B, C). Scale bars = 10 μm.

microscopically (minimum 600 cells). T-test statistic was used to compare *Cryptomonas* cell count of treatment versus control.

3. Results

3.1. Morphology and phylogeny of the strains

A total of thirty-two strains of one diatom and ten dinoflagellate species of potentially toxigenic plankton were obtained during the PHYCOB 2021 cruise (Table 1). Two additional strains of the potentially toxigenic genus *Amphidoma* representing a new species have been described elsewhere (Tillmann et al., 2025).

3.1.1. Diatoms

3.1.1.1. Pseudo-nitzschia calliantha. Two strains of *Pseudo-nitzschia* were obtained at station 19. In light microscopy, cells of both strains were of identical morphology and had a slightly sigmoid cells shape (Fig. 2). Cells were about 70 μm in length (measurements of both strains: 62.0 (68.7) 78.0 μm; $n = 30$) and 3 μm in valve width (2.5 (3.0) 3.6 μm; $n = 30$). Both strains were lost before SEM and/or TEM ultrastructural confirmation of the species designation could be obtained. However, sequence data identified both strains (having 100 % identical LSU rDNA sequences and 99.5 % identical ITS rDNA sequences, due to some ambiguous bases) as *Pseudo-nitzschia calliantha* Lundholm, Moestrup & Hasle. The LSU rDNA sequences of the Black Sea strains were 100 % identical to numerous *P. calliantha* sequences from different locations, including Australia, Slovenia, and Spain. The highest BLAST similarity (99.87 %) for the ITS sequences was with *P. calliantha* strains from the Sea of Japan (GenBank accession numbers: KT247436 and KT247434).

3.1.2. Dinoflagellates

Most of the strains of potentially toxigenic species were members of the Gonyaulacales, with seven strains of *Alexandrium*, six strains of

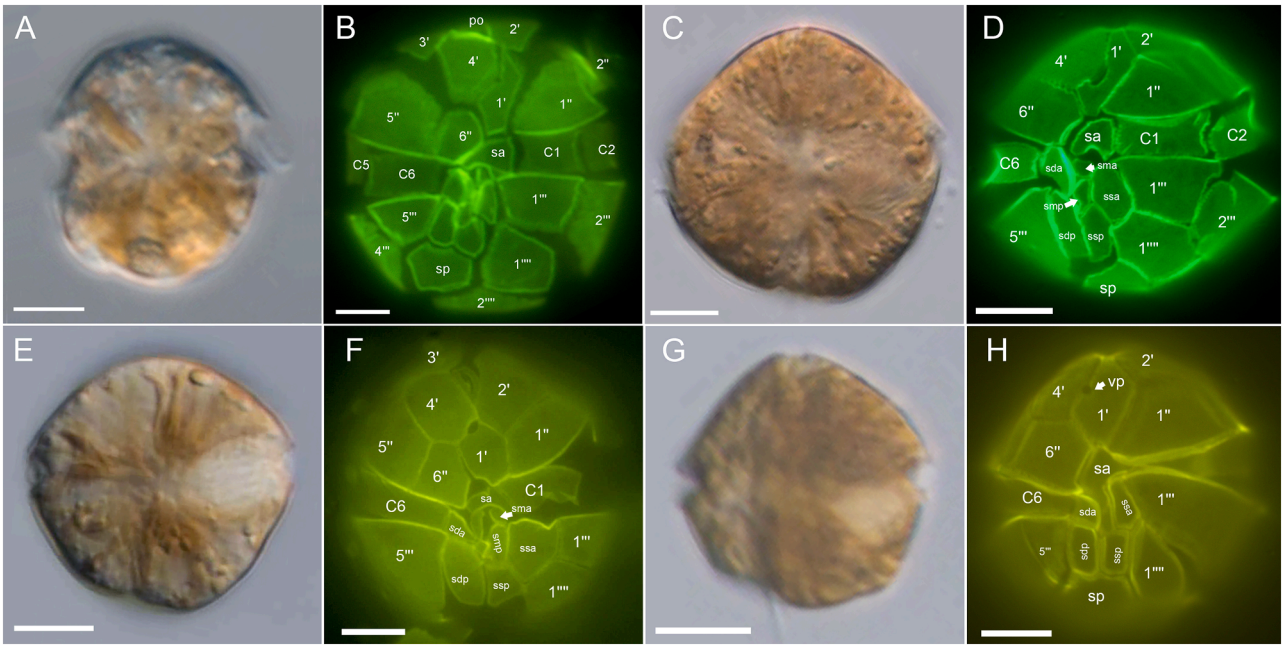

Fig. 3. *Alexandrium* spp., light microscopy images of living cells (A, C, E, G) and lugol fixed cells stained with Solophenyl Flavine and viewed with epifluorescence and green light excitation (B, D, F, H). (A, B) *Alexandrium andersonii* strain BS 5-E11. (C, D) *Alexandrium ostenfeldii* strain BS 5-D3. (E, F) *Alexandrium pseudogonyaulax* strain BS 6-D1. (G, H) *Alexandrium tamutum* strain BS 5-C7. Plate labels according to the Kofoidean system. Sulcal plate labels: sa, anterior sulcal plate ssa, left anterior sulcal plate; ssp, left posterior sulcal plate; sda, right anterior sulcal plate; sdp, right posterior sulcal plate; sma, median anterior sulcal plate; smp, median right sulcal plate; sp, posterior sulcal plate. Scale bars = 5 μm (A, B) or 10 μm (C–H).

Protoceratium reticulatum (Claparède & Lachmann) Bütschli, twelve strains of *Lingulaulax polyedra* Head, Mertens & Fensome, one strain of *Gonyaulax* sp., and one strain of *Sourniaea diacantha* (Meunier) H.Gu, K. N.Mertens, Zhun Li, H.H.Shin. In addition, two strains of the potentially toxigenic gymnodinoid genus *Karlodinium* were obtained.

3.1.2.1. Alexandrium andersonii. One strain (BS 5-E11) isolated at station 11 was identified as *Alexandrium andersonii* Balech (Fig. 3A, B, Suppl. Fig. S1). Cells were small (cell length: 16.6 (20.7) 24.1 μm; cell width: 14.5 (18.1) 21.6 μm; $n = 50$), oval in outline in ventral view, with a slightly submedian cingulum. The orange-brown plastids were mainly concentrated in the posterior part of the cell, whereas the large and conspicuous nucleus was located in the episome (Fig. 3A). The detailed examination of the thecal plate tabulation (Fig. 3B, Suppl. Fig. S1) revealed a consistently present ventral pore on the left suture of the first apical plate (1') and a characteristically shaped anterior sulcal plate (Fig. 3B, Suppl. Fig. S1).

For the ITS sequence of strain BS 5-E11, the highest BLAST similarity was 99.64 % with *A. andersonii* ICMB222 strain from the Catalan Sea (GenBank accession number: HE574398), whereas the LSU sequence was identical (excluding one ambiguous base) to strains from the USA (GenBank accession numbers: KX599343, JF521620, JF521619) and Italy (GenBank accession number: JF521621).

Based on ITS rDNA sequences, the *A. andersonii* clade was subdivided into three well-supported groups, one of which was further divided into two additional well-supported subgroups (Fig. 4). The Black Sea BS 5-E11 strain was placed within the largest group, which contained strains from various locations.

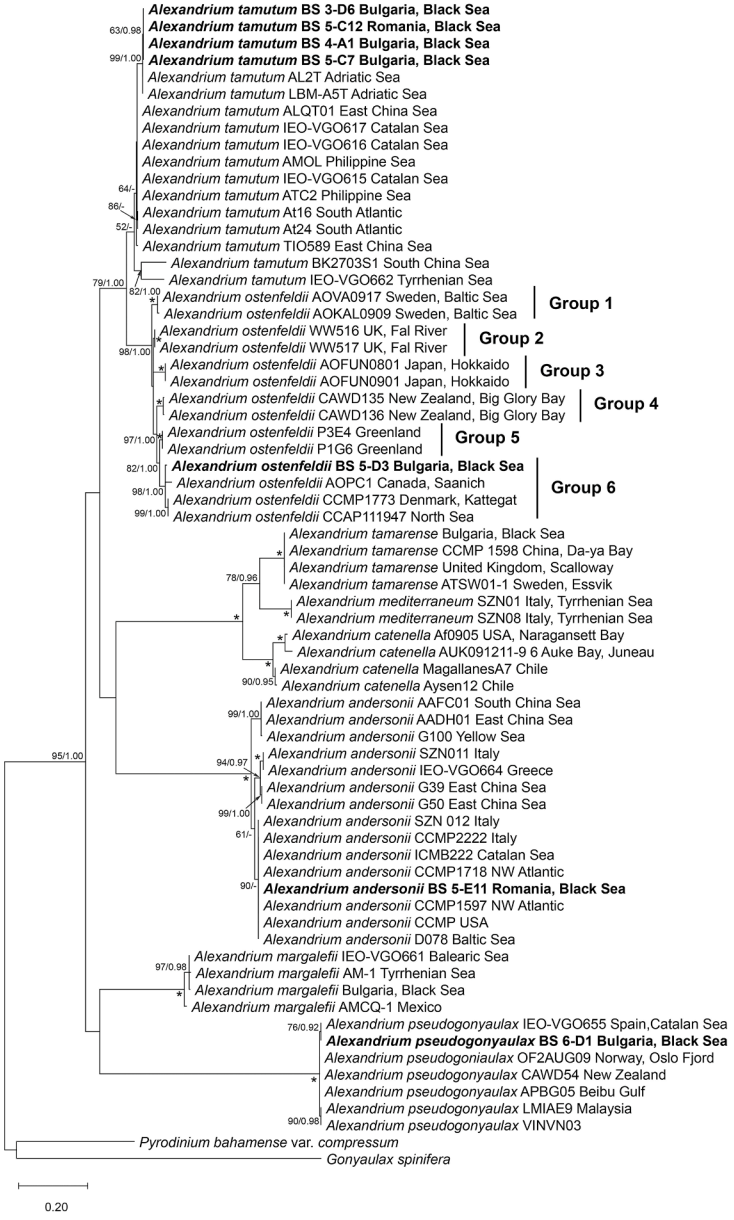

Fig. 4. A maximum likelihood tree derived from an ITS rDNA alignment, including sequences of *Alexandrium* species, with *Pyrodinium bahamense* var. *compressum* and *Gonyaulax spinifera* serving as outgroup taxa. The tree is drawn to scale, with branch lengths measured in substitutions per site. Node labels represent bootstrap values from the maximum likelihood method and posterior probabilities from the Bayesian inference analyses (ML/BI); only bootstrap values >50 % and posterior probabilities >0.9 are shown. The sequences from the current study are indicated in bold. * indicates maximal support, defined as 100 % ML bootstrap support and a Bayesian posterior probability of 1.00. *Alexandrium ostenfeldii* group assignments follow Kremp et al. (2014).

3.1.2.2. Alexandrium ostenfeldii. Strain BS 5-D3, isolated at station 15, was identified as *Alexandriun ostenfeldii* (Paulsen) Balech & Tangen (Fig. 3C, D, Suppl. Fig. S2). The cells were variable in size (cell length: 23.2 (32.5) 45.2 μm; $n = 40$). Cell shape was mostly round with a cell width (24.0 (32.6) 44.3 μm; $n = 40$) similar to cell length. Thecal plate examination revealed the typical plate tabulation of *Alexandrium* and the thecal features characteristic for *A. ostenfeldii*, i.e., the characteristically shaped first apical plate with a conspicuously large oval ventral pore (Fig. 3D, Suppl. Fig. S2E, F). The anterior sulcal plate was slightly variable in shape but mostly had a typical A-shape (Fig. 3D, Suppl. Fig. S2F, J, L).

For both ITS and LSU sequences of strain BS 5-D3, no 100 % identical sequences were found in the GenBank database. For the ITS sequence, even the highest BLAST similarity was under 99 % (98.72 % with *Alexandrium ostenfeldii* strain from Peru, identified as *A. peruvianum*, GenBank accession number: JX841265). In contrast, the LSU sequence differed by only 2 bp from strains from the USA (GenBank accession number: LC433663) and Norway (GenBank accession number: JF521637).

In the phylogenetic tree, *A. ostenfeldii* strain from the Black Sea (BS 5-D3) clustered with *A. ostenfeldii* strains from various geographic locations (ML 98 %, BI 1.00), within Group 6 as defined by Kremp et al. (2014) (Fig. 4).

3.1.2.3. Alexandrium pseudogonyaulax. One of the *Alexandrium* strains (BS 6-D1), isolated at station 19, was identified as *A. pseudogonyaulax* (Biecheler) Horiguchi ex K.Yuki & Y.Fukuya (Fig. 3E, F, Suppl Fig. S3). Cells were variable in size (cell length: 29.7 (41.1) 51.1 μm, cell width: 31.5 (40.8) 52.7 μm; $n = 30$). Cell shape ranged from very slightly compressed to round (Fig. 3E, F), or even slightly longer than wide (Suppl. Fig. S3E), with a mean length/width ratio of 1.01 ± 0.04 ($n = 30$). In growing cultures, the characteristic division cysts (Suppl. Fig. S3F, G) with up to four cells inside were present, whereas sexual cysts (hypnozygotes) were encountered in old dense cultures (Suppl. Fig. S3I). No clear indication of a paratabulation on the surface of these hypnozygotes could be detected (Suppl. Fig. S3I). Occasionally, pairs of cells were observed resembling early stages of gamete fusion (Suppl. Fig. S3H), but their further development was not followed. The species identification of strain BS 6-D1 was supported by the shape and position of the first apical plate 1', which was disconnected from the pore plate (po), by the shape and position of the ventral pore on the suture of plates 1' and 4' (Fig. 3F), and by the shape of the left posterior sulcal plate (ssp) which had a broad base and was as long as wide (Fig. 3F, Suppl. Fig. S3K, O, P).

The ITS rDNA sequence of *A. pseudogonyaulax* strain BS 6-D1 was identical to sequences from two strains from Spain, Catalan Sea (GenBank accession numbers: AM237416 and AM237417). For the LSU sequence, the highest BLAST similarity was 99.4 % (due to four ambiguous bases in the query sequence) with several strains from various geographic locations, including Malaysia, China, Norway, and Japan. Based on the ITS rDNA sequences, BS 6-D1 strain was placed in the well-supported *A. pseudogonyaulax* clade, comprising strains from various geographic locations (Fig. 4).

3.1.2.4. Alexandrium tamutum. Four of the *Alexandrium* strains, which were isolated at stations 3, 10, and 15, were *A. tamutum* Montresor, John & Beran (Fig. 3G, H, Suppl. Fig. S4) These four strains were of similar size and shape (cell length: 23.0 (27.3) 34.3 μm, cell width: 21.6 (25.2) 31.6 μm; $n = 40$). Cell shape was round to oval with a mean length/width ratio of 1.08 ± 0.03 ($n = 40$). The species identification was based on the presence of a ventral pore on the left side of plate 1' (which was consistently present), on a much wider than long plate 6'', and on the shape of the posterior sulcal plate, which was wider than long (Fig. 3H, Suppl. Fig. S4C–H).

All four *A. tamutum* strains had identical ITS rDNA sequences, whereas slight variability was observed in the LSU sequences. The Black Sea strains showed the highest similarity to strains from the Adriatic Sea in the ITS sequence, forming a separate well-supported cluster within

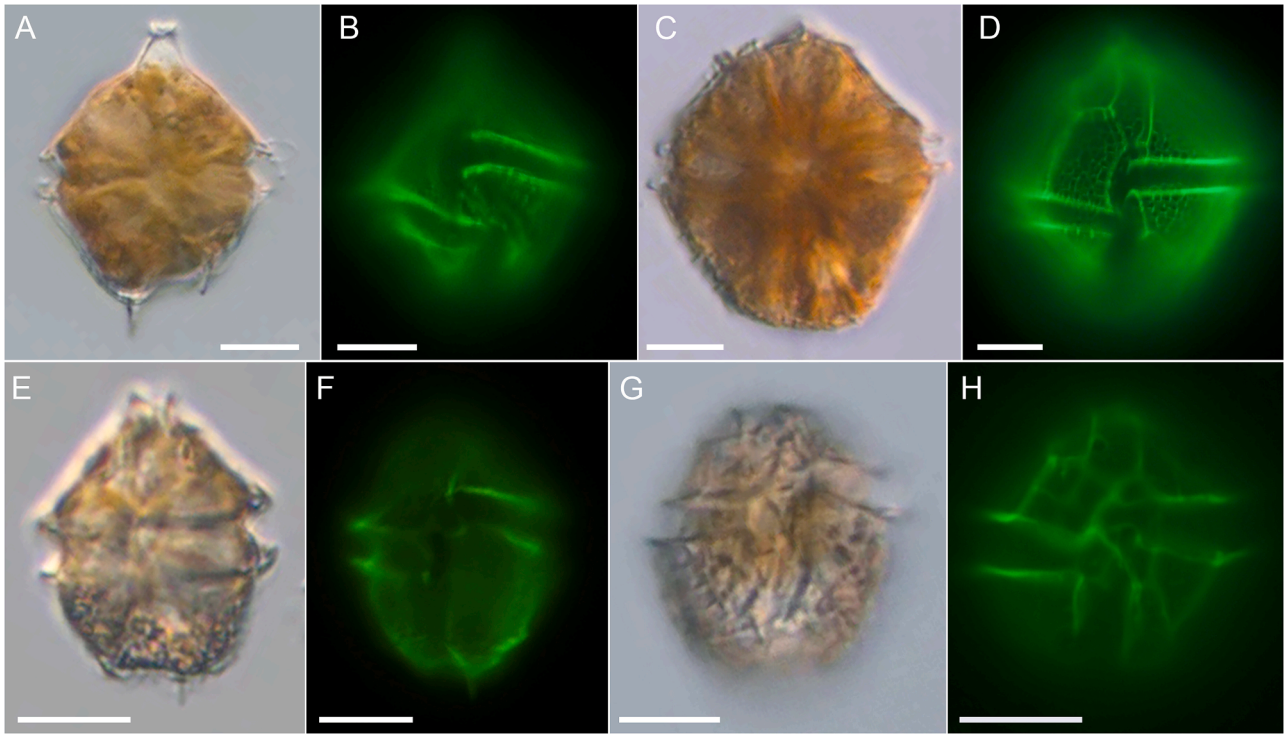

Fig. 5. Gonyaulacalean species, light microscopy images of living cells (A, C, E, G) and lugol fixed cells stained with Solophenyl Flavine and viewed with epifluorescence and green light excitation (B, D, F, H). (A, B) *Gonyaulax* sp. strain BS 5-E4. (C, D) *Lingulaulax polyedra* strain BS 5-C9. (E, F) *Sourniaea diacantha* strain BS 6-D7. (G, H). *Protoceratium reticulatum* strain BS 4-F3. Scale bars = 10 μm (A–D) or 5 μm (E–H).

the *A. tamutum* clade (Fig. 4).

3.1.2.5. Gonyaulax sp.. One strain of *Gonyaulax* sp. was isolated at station 19 (Fig. 5A, B, Suppl. Fig. S5). Cells of strain BS 5-E4 ranged in length from 33.4 to 39.3 μm (mean: 36.8 μm; $n = 20$) and in width from 27.1 to 32.6 (mean: 30.1; $n = 20$). The conical episome with shoulders ended in a short extended apical horn, with the angled shoulder on the right cell side being much more distinct. The cingulum was descending and displaced ca. 3 times the cingulum width. There was a distinct overhang of the cingulum, with an angle between the longitudinal cell axis and a line connecting the ends of ca. 30°. The hypotheca was trapezoidal. There were two unequal hypothecal spines, with the spine on the cell's rights side being distinctly longer.

The plate pattern was determined as APC, 3', 2a, 6'', 6''', 2'''' (Suppl. Fig. S5G–L). Cells had a slender, elongated and raised apical pore complex and a distinct ventral pore located on the right side of the cells at the junction of the 3' and 2a plates (Suppl. Fig. S5F). Thecal plates had a reticulate ornamentation with large pores often in lines along the plate margins, whereas the sulcal plates lacked ornamentation and only had a few pores (Suppl. Fig. S5J–L). Hypnozygote cysts were never observed in the cultures.

Both the LSU and ITS sequences obtained from this strain were

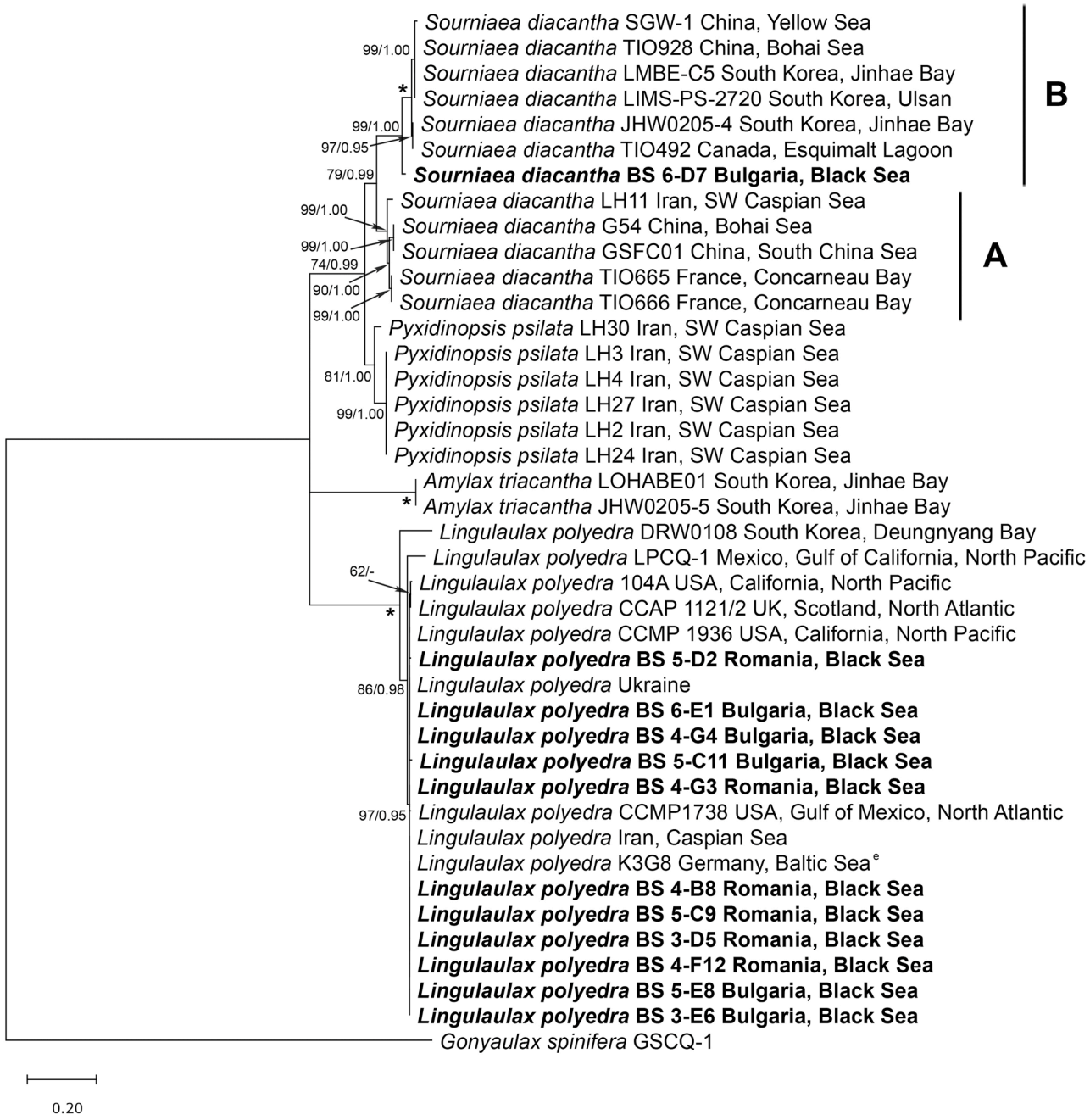

Fig. 6. A maximum likelihood tree derived from an LSU rDNA alignment including sequences of *Sourniaea diacantha, Pyxidinopsis psilata, Amylax triacantha*, and *Lingulaulax polyedra* strains, with *Gonyaulax spinifera* serving as an outgroup. The tree is drawn to scale, with branch lengths measured in the substitutions per site. Node labels represent bootstrap values from the maximum likelihood method and posterior probabilities from the Bayesian inference analyses (ML/BI); only bootstrap values >50 % and posterior probabilities >0.9 are shown. The sequences from the current study are indicated in bold. * indicates maximal support, defined as 100 % ML bootstrap support and a Bayesian posterior probability of 1.00. *Sourniaea diacantha* group assignments follow Zhang et al. (2020). The index [e] indicates an epitype.

inconclusive, showing low similarity to ribosomal RNA/internal transcribed spacer region sequences in the GenBank database. The strain was lost before new material could be obtained for confirmatory DNA sequencing. As a result, the species identity of this *Gonyaulax* strain remains unresolved.

3.1.2.6. Lingulaulax polyedra. A total of 12 strains of *L. polyedra* (Stein) were isolated at stations 3, 5, 10, 11, 13, 15, 16, 19, and 20 (Table 1). All strains were indistinguishable in cell size and shape and thecal plate details. Cell length (of all strains) was 36.8 (42.6) 54.9 μm ($n = 50$) and cell width (of all strains) was 31.4 (37.7) 45.4 μm ($n = 50$). Exemplarily, cells of strains BS 5-C9 are illustrated in Fig. 5C, D and Suppl. Fig. S6. The cells had the typical heptagonal outlines in ventral or dorsal view and a small, raised apical pore. The hypotheca had a flat antapex without projections. The cingulum was almost median, narrow, displaced without overhang for ca. two cingular widths. In the middle of the suture between plates 1' and 3a, a ventral pore was present (Suppl. Fig. S6I). The surface of thecal plates was coarsely areolate with multiple round structures interconnected by ridges (Fig. 5D, Suppl. Fig. S6E–L).

All examined *L. polyedra* strains had identical ITS sequences, which showed 100 % BLAST similarity to multiple sequences from different geographic locations deposited in the GenBank database (Fig. 6). The Black Sea strains displayed slight variability in the LSU region but were placed within the same cluster, which included all examined strains except the DRW0108 strain from South Korea and the LPCQ-1 strain from Mexico, both of which emerged as separate branches within the *L. polyedra* clade (Fig. 6).

3.1.2.7. Sourniaea diacantha. One strain (BS 6-D7), isolated at station 20, was identified as *Sourniaea diacantha* (= *Gonyaulax verior*) (Fig. 5E, F, Suppl. Fig. S7). Cells of strain BS 6-D7 were longer (23.2 (28.4) 34.8 μm, $n = 30$) than wide (15.2 (21.1) 26.0 μm, $n = 30$) and were markedly compressed dorso-ventrally (Suppl. Fig. S7D, F). Cells had a conical epitheca with straight lines tapering into an apical horn. The hypotheca

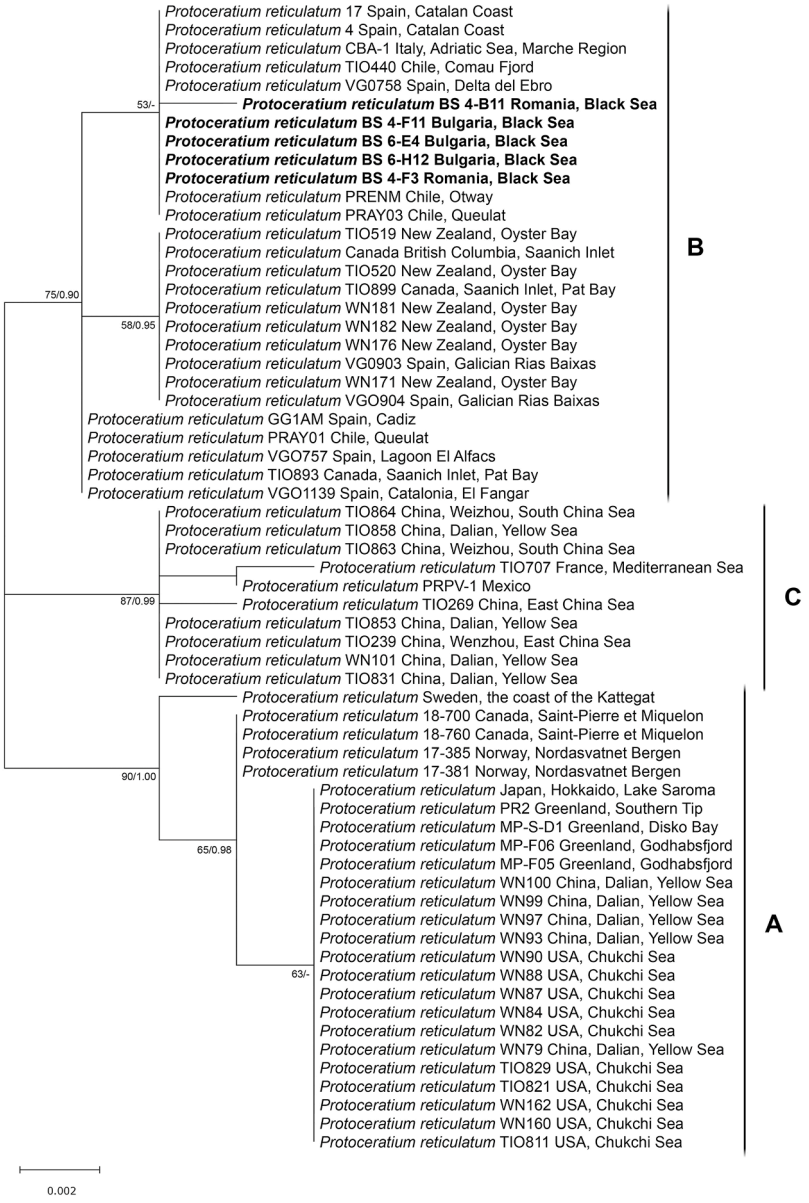

Fig. 7. A maximum likelihood tree derived from an ITS rDNA alignment, including 62 sequences of *Protoceratium reticulatum*. The tree is drawn to scale, with branch lengths measured in the substitutions per site. Node labels represent bootstrap values from the maximum likelihood method and posterior probabilities from the Bayesian inference analyses (ML/BI); only bootstrap values >50 % and probabilities >0.9 are shown. The sequences from the current study are indicated in bold. Group assignments follow Wang et al. (2019). The index [t] denotes the type locality.

was hemispherical with a more or less truncated antapex. The cingulum was descending and displaced without overhang by one girdle width. Cells had one short antapical spine on the left side, which however was often not clearly developed or missing.

The ITS rDNA sequence of strain BS 6-D7 showed significant differences from the reference sequences of *S. diacantha* deposited in the GenBank database. The highest BLAST similarity was 87.67 % to a strain from Canada (GenBank accession number: MT041622). For the LSU sequence, the highest BLAST similarity was 96.06 % to an isolate from Korea, Jinhae Bay (GenBank accession number: EF613349).

In the phylogenetic tree based on LSU rDNA sequences, *S. diacantha* strains formed a monophyletic clade (ML 79 %, BI 0.99), which was subdivided into two well-supported subclades (ML 99 %, BI 1.00) (Fig. 6). The Black Sea strain formed a separate branch that grouped with strong support (ML 99 %, BI 1.00) with the clade referred to as ribotype B (Zhang et al. 2020), which includes strains from China (Bohai Sea), South Korea, and Canada (Esquimalt Lagoon).

The genetic distances between the Black Sea strain BS 6-D7 and the other analyzed strains of *S. diacantha* were high, particularly based on partial ITS alignment (seven sequences, 529 bp), ranging from 12.6 % to 25.5 % (Table S6), and between 4 % and 12 % based on partial LSU sequences (12 sequences, 702 bp) (Table S7).

3.1.2.8. Protoceratium reticulatum. Six strains of *Protoceratium reticulatum* were obtained at stations 2, 5, 11, 19, and 20. All strains shared the same morphology (Fig. 5G, H). Cells were subsphaeroideal and longer than wide, but variable in cell shape and size. The cell length of all strains was 20.7 (25.5) 32.2 μm (n = 40), the cell width was 17.2 (21.8) 25.4 μm (n = 40). The cingulum was located above the median line and was deeply incised and displaced about one cingulum width. The cells had a strongly ornamented theca with raised ridges and numerous pores with a single pore in each of the polygonal

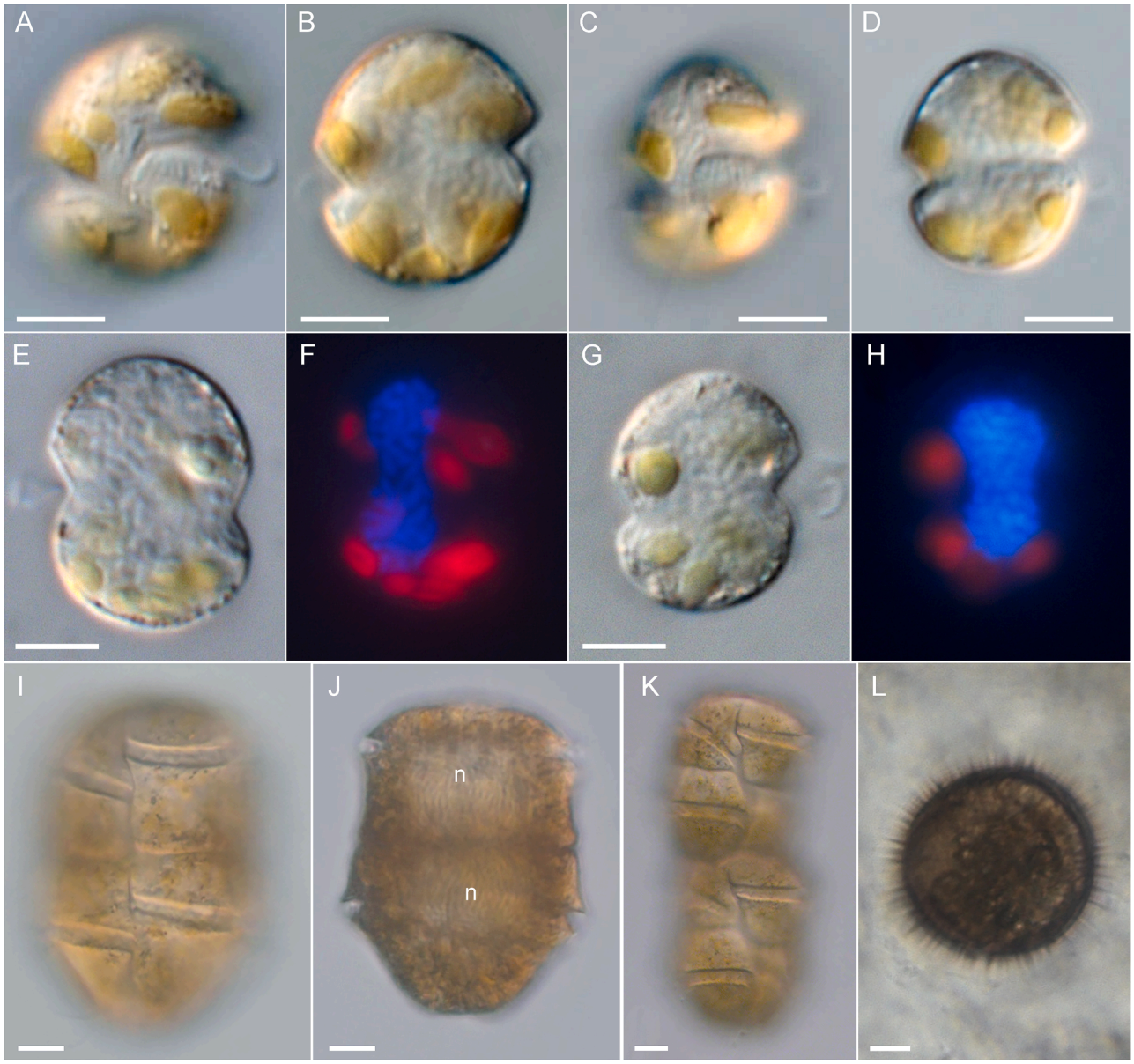

Fig. 8. *Karlodinium* sp. strain BS 3-F8B and *Polykrikos hartmannii* strain BS 7-E9. (A–H) *Karlodinium* sp., light microscopy images of living cells of (A–D) and pair of the same formalin fixed and DAPI-stained cells (E–H) viewed with either regular light (E, G) or UV excitation (F, H) to indicate shape and position of the nucleus (blue) and chloroplasts (red). (I–L) *Polykrikos hartmannii*, light microscopy images of living cells. (I) Pseudocolonie in ventral view. (J) Pseudocolonie in dorsal view. Note the two nuclei (n). (K) Four zoid pseudo-colony just after zoid division. (L) Hypnozygote (resting cysts) as observed not in the clonal strain but onboard in isolation plates where several *P. hartmannii* cells had been collected. Scale bars = 5 μm (A–H) or 10 μm (I–L).

ornamentation. Epifluorescence microscopy revealed the major plate tabulation as APC, 3', 1a, 6'', 6''' and 2'''' (Suppl. Fig. S8). On the first apical plate a large ventral pore was visible. On the epitheca there was one dorsally located intercalary plate clearly disconnected from the pore plate.

All Black Sea *P. reticulatum* strains displayed identical ITS rDNA sequences, except for one strain (BS 4-B11) that showed a transition at three positions (one position within the alignment length). In the phylogenetic tree, *P. reticulatum* strains from the Black Sea clustered with a clade (ML 75 %, BI 1.00) defined as "ribotype B" by Wang et al. (2019), which included strains from temperate regions (Fig. 7). Strains from the type locality (Norway, Bergen) were positioned within clade A. The Swedish strain (the coast of the Kattegat) grouped with clade A with high support (ML 90 %, BI 1.00), in contrast to the findings of Wang et al. (2019), where it was placed outside the clades.

All examined *P. reticulatum* strains had identical LSU rDNA

Fig. 9. A Maximum Likelihood tree derived from a concatenated ITS/LSU alignment, including sequences of *Karlodinium, Karenia*, and *Takayama* species, with *Gymnodinium aureolum* and *Gymnodinium catenatum* serving as an outgroup. The tree is drawn to scale, with branch lengths measured in the number of substitutions per site. Node labels represent bootstrap values from the maximum likelihood method and posterior probabilities from the Bayesian inference analyses (ML/BI); only bootstrap values >50 % and posterior probabilities >0.9 are shown. The sequences from the current study are indicated in bold. * indicates maximal support, defined as 100 % ML bootstrap support and a Bayesian posterior probability of 1.00. The sequences from the current study are indicated in bold. *Karlodinium* group assignments follow Benico et al. (2020). The index [h] denotes the holotype.

sequences, showing 100 % similarity to numerous GenBank reference sequences from diverse geographic locations, including isolates representing all three ribotypes.

3.1.2.9. Karlodinium sp. Two strains of the gymnodinoid genus *Karlodinium* (strain BS 3-F8B and BS 6-E10) were isolated at station 2 and 15. Both strains were indistinguishable in light microscopy, and were slightly longer (10.7 (13.4) 14.7 µm, $n = 40$) than wide (8.3 (11.0) 12.8 µm, $n = 40$). Strain BS 3-F8B was selected to be depicted in detail (Fig. 8A–H). Cells were ovoid in outline and only slightly compressed dorsoventrally (Fig. 8A–D). The epicone was conical with the straight apical groove and the ventral pore at times discernible (Fig. 8C). The hypocone was hemispherical and of less height compared to the epicone. The cingulum was excavated, descending and displacing ca. 1/3 to 1/4 of the cell length. In LM there was no marked extension of the sulcus into the episome visible. The sulcus was wide posteriorly in the hypocone, but became narrow in the intercingular region. The large nucleus was elongated (Fig. 8E–H) and located in the left side of the cell, as evident from a specimen with an unambiguous ventral orientation (Fig. 8A, B). There were ca. 5–8 irregularly shaped, orange chloroplasts distributed at the cell periphery.

Both examined *Karlodinium* strains displayed identical ITS and LSU rDNA sequences. The highest BLAST similarity for the ITS sequence was 95.30 % with *Karlodinium ballantinum* strains (GenBank accession numbers: PP616686 and LC521285), while for the LSU sequence it was 98.66 % with *Karlodinium gentienii* (GenBank accession number: KJ508379). The genetic distances between the Black Sea strains of *Karlodinium* sp. and the analyzed strains of other *Karlodinium* species were relatively high based on the partial ITS alignment (26 sequences, 643 bp), ranging from 4.9 % to 22.2 % (Table S8), and lower based on LSU sequences (35 sequences, 757 bp), ranging from 1.3 % to 11 % (Table S9).

In the concatenated phylogenetic tree, *Karlodinium* species were divided into three distinct clades with high support values. The two Black Sea *Karlodinium* strains clustered in a single branch (ML 100 %, BI 1.00), nested within the largest clade (Clade 1) (ML 96 %, BI 1.00), which contained several subclades (Fig. 9). The Black Sea *Karlodinium* strains were related to a cluster that includes *K. zhouanum, K. jejuense*, and an unidentified (at the species level) *Karlodinium* isolate from South Korea (*Karlodinium* sp. KAMS0708).

3.1.2.10. Polykrikos hartmannii. Finally, one strain of *Polykrikos hartmannii* was obtained (Fig. 8I–L). The pseudocolonies consisted of two zoids, whose separation was clearly visible due to a constriction in the middle of the pseudocolony. The size of the two zoid pseudocolonies was 61.8 (76.0) 93.7 µm in length ($n = 50$) and 37.7 (49.9) 61.8 µm in width ($n = 50$). Rarely, single zoids were also present in the cultures. The two zoid pseudocolonies had two nuclei and were brownish in color due to the chloroplasts. The cingulum of each zoid was descending and displaced for about three cingular width. After the division of both zoids, short chains of four zoids were temporarily formed (Fig. 8K), which soon split into two pseudocolonies. In the onboard isolation plates, where several *P. hartmannii* pseudocolonies had been collected, resting cysts were observed (Fig. 8L), whereas such stages were no longer observed later in the clonal culture. The cysts were round and densely covered with short, pointed spines. The LSU rDNA sequence of the Black Sea

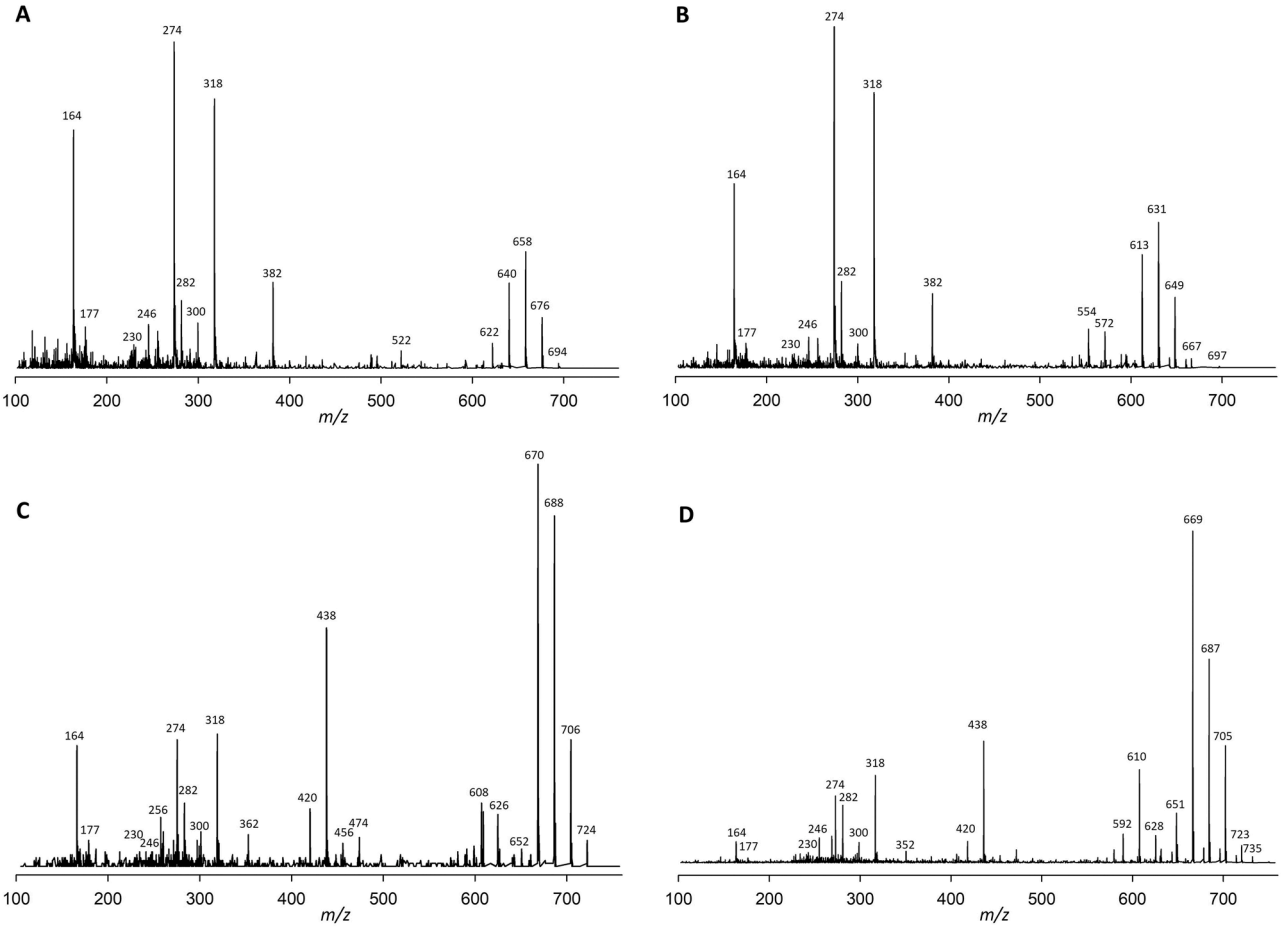

Fig. 10. Collision-induced (CID) spectra of the four novel spirolides (SPX) detected in the *A. ostenfeldii* strain BS 5-D3 from the Black Sea. A) Compound 1 (SPX *m/z* 694), B) Compound 2 (SPX *m/z* 697), C) Compound 3 (SPX *m/z* 724), and D) Compound 4 (SPX *m/z* 753).

strain of *P. hartmannii* (BS 7-E9) was identical to multiple reference sequences from the GenBank database originating from various geographic locations, including China, Korea, Canada, and the USA. For the ITS rDNA sequence, no comparison was possible due to the absence of sequences in the database.

3.2. Toxin profiles and cell quotas

The two strains (BS 3-F11 and BS 4-H4) of *Pseudo-nitzschia calliantha* were analyzed for domoic acid (DA), but no detectable levels above the LOD were found (LOD values of DA: 6.0 and 8.3 fg cell^{-1} for strains BS 3-F11 and BS 4-H4, respectively).

All strains of *Alexandrium* spp. (four strains of *A. tamutum*, one strain of each *A. andersonii, A. ostenfeldii* and *A. pseudogonyaulax*) were analyzed for all toxins known to be produced by the genus, i.e., PSTs, goniodomins, and cycloimines (gymnodimines and spirolides). None of the strains contained detectable levels of PSTs (for detection limits, see Table S12), and gymnodimines. Instrumental detection limits of the analyzed phycotoxins and used injection volumes are given in Table S13. Only the *A. pseudogonyaulax* strain contained GDA and GDA-sa at cellular levels of 14.0 and 0.33 pg cell^{-1}, respectively. Collision induced dissociation (CID) experiments showed evidence of four yet unreported SPX analogues (Fig. 10) of the *A. ostenfeldii* strain BS 5-D3; cell quotas expressed as SPX-1 equivalents ranged between 1.0 and 1.6 pg cell^{-1}. The LOD values (S/N = 3) for gymnodimine, goniodomin and spirolide analyses are compiled in Table S14. The m/z values and retention times of the four novel SPX were: Cp 1: 694, 10.61 min; Cp 2: 697, 8.89 min; Cp 3: 724, 10.81 min; and Cp 4: 753, 10.23 min. The high-resolution mass data of Cp 1–4 of and their major fragments are given in Table S15-A to -D.

Both strains of *Karlodinium* sp. (BS 6-E10 and BS 3-F8B) were investigated for KmTx-related compounds but neither contained detectable levels of currently known KmTx. The LOD values of KmTx were determined as 1.0 and 2.2 fg cell^{-1} for strain BS 6-E10 and BS 3-F8B, respectively.

All 20 strains of the potentially YTX producing species (*Gonyaulax* sp., *Sourniaea diacantha, Protoceratium reticulatum, Lingulaulax polyedra*) were analyzed for yessotoxins. No YTXs were detected in the strains of *Gonyaulax* sp. (BS 5-E4) and *S. diacantha* (BS 6-D7), whereas all six strains of *Protoceratium reticulatum* contained YTX with cell quotas ranging between 1.9 and 5.4 pg cell^{-1} (Table S16). In nine of the twelve strains of *Lingulaulax polyedra* several YTX variants were detected (Table S17), but none of the strains contained YTX. The most abundant YTX congener was 45-hydroxy-1a-homoYTX (mass transition m/z 1171 → 1091) followed by 9-Me-41a-homo-YTX (mass transition, m/z 1169 → 1089), trinor-YTX (mass transition m/z 1101 → 1021), and the compounds 21, 22 (mass transition m/z 1061 → 981) reported by Miles et al. (2005a, 2005b). In addition to these compounds, five other putative YTXs could be detected at trace levels: m/z 1173 →1093 (Carboxy-YTX), m/z 1131 → 1051 (undescribed), m/z 991 → 911 (compound 17, Miles et al. 2005a, 2005b), m/z 1195 → 1115 (undescribed) and m/z 1887 → 1807 (undescribed). The limit of detection (LOD) of YTX are listed in Table S18.

Both strains of *Karlodinium* and the single strain of *Polykrikos hartmannii* were tested for potential lytic activity towards the cryptophyte *Cryptomonas salina*. The cell densities of the donor strains were 135 × 10^3 and 92 x × 10^3 cells mL^{-1} of *Karlodinium* strain BS 6-E10 and BS 5-F8B, respectively, and 0.43 × 10^3 cells mL^{-1} of *P. hartmannii* strain BS 7-E9. All three strains did not show any signs of lytic activity in the 24 h incubation period, i.e. *Cryptomonas* cell densities of treatment and control were not significantly different (T-test: $p > 0.3$).

4. Discussion

In the present work, the use of newly isolated cultures of a number of potentially toxic species from the Black Sea allowed for the first time a detailed phylogenetic and toxinological characterization, in addition to a morphological description, of these species. Such data allow for a better understanding and explanation of the sources and dynamics of phycotoxins in water samples and marine organisms along the food chain from the region.

4.1. Pseudo-nitzschia

In the Black Sea, blooms of the diatom genus *Pseudo-nitzschia* (Mikaelyan, 1995; Bodeanu, 2002; Türkoğlu and Koray, 2002; Terenko and Terenko, 2012) and the presence of their toxin (domoic acid) in shellfish (Peneva et al., 2011; Peteva et al., 2018) are of concern (Dzhembekova et al., 2021). *Pseudo-nitzschia* is a common component of the marine plankton in the Black Sea, with bloom densities reaching > 10^6 cells L^{-1} in various offshore and coastal areas (Bodeanu, 2002; Ryabushko, 2003b). In the Black Sea, *Pseudo-nitzschia calliantha* is the only species confirmed to produce domoic acid, with a single strain from Sevastopol Bay having DA levels ranging from 0.1 to 1 pg cell^{-1} (Besiktepe et al., 2008). A total of eight other *Pseudo-nitschia* species known to be potentially DA producers are described from the Black Sea (reviewed by Dzhembekova et al., 2021), but the toxin production of their local populations has not been confirmed yet. Both new *Pseudo--nitzschia* strains presented here are *P. calliantha*, but DA production in our cultures could not be confirmed. This finding matches the field data from the survey, where no DA was found in plankton samples (Dzhembekova et al., 2025). As it is known for a number of *Pseudo--nitzschia* species (reviewed in Lelong et al., 2012; Bates et al., 2018), both toxigenic (Martin et al., 1990) and non-toxigenic (Lundholm et al., 2003) strains of *P. calliantha* have been described in the literature. Thus, our results indicate that both toxigenic and non-toxigenic strain types may co-occur in the Black Sea. However, several studies have shown that DA production is modulated by various environmental factors (reviewed in Lelong et al., 2012; Bates et al., 2018), even if *Pseudo-nitzschia* strains carry the *dab* gene cluster involved in the biosynthesis of this neurotoxin (He et al., 2024). Unfortunately, both new Black Sea *P. calliantha* strains were lost before it could be tested if other growth conditions such as silicate limitation and/or e.g., exposure to copepod cues may elevate DA production above LOD levels.

4.2. Alexandrium spp.

There are quite a number of species of *Alexandrium* listed in various plankton checklists of the Black Sea (Gómez and Boicenco, 2004; Moncheva and Parr, 2015; Krakhmalny et al., 2018). However, their diversity remains poorly documented, as morphological evidence for most of these species is not available. In fact, references in these lists substantiating records of *Alexandrium* species in the Black Sea almost exclusively refer to other undocumented checklists, to unavailable grey literature, or to papers lacking descriptions or illustrations. Whereas the annotated checklist of dinoflagellates of the Black Sea by Gómez and Boicenco (2004) includes two species of *Alexandrium,* with *A. ostenfeldii* considered as a valid record and *A. monilatum* ranked as questionable /dubious species in the area, another checklist (Krakhmalny et al., 2018) includes seven *Alexandrium* species (*A. affine, A. catenella, A. minutum, A. monilatum, A. ostenfeldii, A. pseudogonyaulax, A. tamarense*). In recent metabarcoding studies, the presence of additional *Alexandrium* species, such as *A. andersonii, A. margalefii*, and *A. tamutum*, has been discussed based on short SSU sequences (Dzhembekova et al., 2022). Additionally,

A. margalefii and *A. tamarense* were identified in Bulgarian waters based on ITS and LSU data obtained from single-cell PCR (GenBank accession numbers: PV242896, PV242897, PV252065, and PV252064, unpublished data). However, very little morphological evidence of these species has been reported for the Black Sea so far. With the strain-based data presented here, we now substantially contribute to the discussion on *Alexandrium* diversity in the Black Sea.

4.2.1. *Alexandrium andersonii*

Thus, we now provide the first morphological evidence of *A. andersonii*, supported by long rDNA sequences, thereby validating the first metabarcoding-based indication of the presence of this species in the Black Sea (Dzhembekova et al., 2022). The species is small and inconspicuous, making it difficult to identify under a light microscope. It has likely been overlooked until now and was also not reliably identified as such in our live observations on board during the PHYCOB cruise. This highlights the strength of the strain-establishment approach, which enables clear identification through morphology supported with long sequences. Moreover, it allows the determination that *A. andersonii* from the Black Sea (although tested here with only a single strain) does not produce any of the toxins known of *Alexandrium*. Measurements on the potential production of cycloimines (spirolides and gymnodimines) have never been conducted on strains of this species before. This is therefore the first solid indication that this species does not produce these substances. Regarding the PST production potential of *A. andersonii,* different reports exist in the literature. While Ciminiello et al. (2000) reported PSTs (STX and NEO) in the Mediterranean strain SZN12 of *A. andersonii*, a subsequent study by Frangopulos et al. (2004) using the same strain, reported very low levels of mainly GTX-2. In any case, Sampedro et al. (2013) convincingly demonstrated that the same strain SZN12, along with four other strains of *A. andersonii*, did not produce any PSTs, discussing methodological issues that may have led to the positive PST findings reported earlier (Ciminiello et al., 2000; Frangopulos et al., 2004). A general absence of PST production in *A. andersonii* is further supported by data of strains from Massachusetts, USA (Orr et al., 2011), a strain from the Irish Sea (Touzet et al., 2007), and our results for the Black Sea strain. Additionally, Stüken et al. (2011) confirmed this by failing to detect genes required for STX synthesis in two strains of *A. andersonii*. Nevertheless, *A. andersonii* is known to be mixotroph (Lee et al., 2016) producing unknown bioactive metabolites that cause hemolysis (Sampedro et al., 2013) and/or cytotoxicity (Sansone et al., 2018). Therefore, the occurrence, distribution, and potential blooms of this species in the Black Sea should be carefully monitored in the future.

4.2.2. *Alexandrium tamutum*

While none of the seven *Alexandrium* strains presented here belong to *A. minutum, A. tamutum* is the most frequently (four out of a total of seven strains) isolated *Alexandrium* species during the PHYCOB cruise, suggesting that *A. tamutum* is the dominant *Alexandrium* in the autumn communities in the area. Consistently, the species was detected at ten stations based on DNA metabarcoding (Dzhembekova et al., 2025). This is particularly significant because *A. tamutum* bears a strong resemblance to *A. minutum*, an important PST-producing species that appears on various plankton lists for the Black Sea. However, many records of *A. minutum* in the Black Sea lack convincing and definitive descriptions or photographic documentation. There is a light microscopy image labeled as *A. minutum* in Krakhmalnyi et al. (2024). However, since neither the 6'' plate nor the surface structure of the hypotheca is clearly visible, it is impossible to determine with certainty which *Alexandrium* species this actually represents. Particularly interesting SEM images appears in Vershinin et al. (2006; their Fig. 4a) and Vershinin and Velikova (2008; their Fig. 14), which convincingly show cells with a narrow 6'' plate. There is no doubt that these cells have a reticulated hypotheca, similar to cells identified as *A. minutum* by Montresor et al. (1990) in samples from Naples. However, this classification was made before the recent description of *Alexandrium fragae* (Branco et al., 2020). This species closely resembles *A. minutum* but is specifically characterized by an areolate hypotheca, so that the cells from the Gulf of Naples (Marina Montresor, pers. comm.) and also the cells depicted by Vershinin et al. (2006) and Vershinin and Velikova (2008) are likely to be *A. fragae*. In SEM images of field samples from the PHYCOB 2021 cruise, a similar observation was made (Dzhembekova et al., 2025), suggesting that *A. fragae* might be - at least partly - responsible for PSTs in the Black Sea. In terms of PST profile, *A. fragae* produce predominantly gonyautoxins (GTX-2/3) with low levels of saxitoxin, which also conform with the finding of GTX-2/3 in shellfish from the Black Sea (Vershinin et al., 2006; Kalinova et al., 2015; Peteva et al., 2020) and their detection in plankton samples from the PHYCOB 2021 cruise (Dzhembekova et al., 2025).

While *A. minutum* is listed on Black Sea plankton check lists, the new strains of *A. tamutum* reported here are the first records of this species for the Black Sea. Since *A. tamutum* was originally described from the Mediterranean (Montresor et al., 2004), its presence in the Black Sea is not particularly surprising. Molecular phylogenetic analyses show that the Black Sea strains form a clade with two Adriatic strains, although ITS rDNA subclades reflect genetic variability rather than geographic origin (Menezes et al., 2018).

As has been demonstrated for multiple strains from various regions (Long et al., 2021; and references therein), *A. tamutum* does not produce PSTs, which has now also been confirmed with multiple strains from the Black Sea. Additionally, the current analyses show for the first time that *A. tamutum* does not produce cycloimines or goniodomins.

4.2.3. *Alexandrium pseudogonyaulax*

Cells of *A. pseudogonyaulax* are generally characterized by significantly wider than long cell shape, but cells of the strain from the Black Sea in culture tend to be more rounded. In this regard, the Black Sea *A. pseudogonyaulax* aligns with strains from the Limfjord, which also show high variability in cell shape in culture and are mostly rounded (Kremp et al., 2019). This makes it very difficult, if not impossible, to easily distinguish *A. pseudogonyaulax* from the closely related species *A. hiranoi*, which is generally described with a more round shape compared to *A. pseudogonyaulax* (Kita and Fukuyo, 1988). Based on LSU and SSU sequences, the two species cannot be distinguished, meaning that metabarcoding records, such as those reported from the PHYCOB cruise (Dzhembekova et al., 2025), do not allow for a clear species-level identification. However, the morphological analysis of strain BS 6-D1 clearly identifies it as *A. pseudogonyaulax*, particularly based on the characteristic shape of the left posterior sulcal plate (Suppl. Fig. S3). In *A. pseudogonyaulax*, this plate is flat and broader at the base, whereas in *A. hiranoi*, it is elongated and narrower at the base compared to the apical end (Kita and Fukuyo, 1988). From a toxinological perspective, *A. pseudogonyaulax*, as all species within the phylogenetically defined *Gessnerium* clade (Abdullah et al., 2023), is significant as a producer of goniodomins (GD) (Zmerli Triki et al., 2014). Our measurements confirm that the strain from the Black Sea, like most other *A. pseudogonyaulax* strains studied so far, produces GDA but does not produce PST and/or cycloimines. The identification of *A. pseudogonyaulax* thus complements the record of GDA at three stations of the PHYCOB cruise (Dzhembekova et al., 2025) indicating that indeed *A. pseudogonyaulax* is the source of GD in the Black Sea. Goniodomin has biological effects (e.g. cytotoxic to mice: (Terao et al., 1989)) and ichthyotoxic blooms of *A. monilatum*, another GD producer, are known (May et al., 2010), although recent studies suggest that a broad spectrum of effects of *A. pseudogonyaulax* on other marine organisms may be more attributable to undefined bioactive substances rather than GD (Gaillard et al., 2024; Möller et al., 2024). In any case, there is a need to closely monitor the development of this species in the Black Sea. Another GD producing species, *Alexandrium monilatum* (the type species of the *Gessnerium* group), is also included in various lists of HAB species of the Black Sea (Moncheva and Parr, 2015; Krakhmalny et al., 2018),

and is even listed as having formed blooms $>10^6$ cells per liter (Moncheva et al., 2001). However, neither morphological descriptions/documentation nor sequence indication for such records are available and we thus agree with Gómez and Boicenco (2004) that these records are dubious and convincing evidence is still needed to unambiguously confirm the presence of *A. monilatum* in the Black Sea.

4.2.4. *Alexandrium ostenfeldii*

This is the only species of *Alexandrium* considered to be reliably documented for the Black Sea in the checklist by Gómez and Boicenco (2004). However, even a widely cited record of a bloom of this species in 2005 in Sozopol Bay is based solely on a one-page abstract without any supporting documentation (Mavrodieva et al., 2007). Since *A. ostenfeldii* is known from other regions as a producer of PST, the question arises whether local populations in the Black Sea could be a source of the PST toxins found in Black Sea mussels and field samples (Vershinin et al., 2006; Peteva et al., 2019, 2020). With the first strain from the Black Sea now available, we are able to provide information on this for the first time. The strain BS 5-D3 does not produce PST toxins and is thus - despite the low salinity of the Black Sea - significantly different from previously identified PST-producing *A. ostenfeldii* strains which have mainly been isolated from other brackish water environments, such as the eastern Baltic Sea (Kremp et al., 2009) or brackish estuaries in the USA (Borkman et al., 2012) and the Netherlands (Van de Waal et al., 2015). This is also reflected in the phylogeny, as the BS strain belongs to a different clade (clade 6), comprising strains with no or low cellular concentrations of PSTs (Kremp et al., 2014). Nevertheless, the Black Sea *A. ostenfeldii* strain is quite interesting from a toxinological point of view as here four new spirolide analogues were detected. SPXs are neurotoxins that target nicotinic receptors (Aráoz et al., 2015) and are antagonists to acetylcholine receptors (Nieva et al., 2020a). SPXs are relatively easy to identify by tandem mass spectrometry due to their characteristic CID fragmentation patterns that consist of the cycloimine fragment *m/z* 164 as well as fragments with even *m/z* values (Sleno et al., 2004). Even though unambiguous structural elucidation of organic chemical compounds is only possible by nuclear magnetic resonance (NMR) spectroscopy, in the past SPX structures have successfully been assigned based on CID spectra by the use of analogies between spectra of known and structurally elucidated SPXs and novel SPXs (Nieva et al., 2020b). However, the CID spectra of the four novel SPXs of the Black Sea isolate BS 5-D3 display a completely different fragmentation pattern with the main fragment *m/z* 318 that has not yet been observed in any other SPX with the only exception of compound 9 of one West Greenland *A. ostenfeldii* (Nieva et al., 2020b). Due to the lack of structurally elucidated SPX that produce the *m/z* 318 fragment, a structural assignment of the new SPX is not possible. Nevertheless, the identity of the low mass CID fragments of all four compounds (Fig. 10) indicates a common initial biosynthetic pathway. Interestingly, two of the four new SPXs, have uneven $[M + H]^+$ pseudomolecular ions (Fig. 10B, D), most likely due to the presence of two nitrogen atoms in the molecules. The occurrence of SPXs containing two nitrogen atoms has not yet been observed and underlines the genetic isolation of the Black Sea *A. ostenfeldii* population and supports the hypothetis for the existence of an endogenous *A. ostenfeldii* population in the Black Sea rather than a recent introduction from e.g. the Mediterranean Sea, where different SPX profiles have been reported (Ciminiello et al., 2007; Garcia-Altares et al., 2014; Salgado et al., 2015). It is also noteworthy that Cp 1 and Cp 2 (Fig. 10A, B) were previously detected in planktonic field samples of the Black Sea during a cruise with R/V Akademik in May/June 2019. At that time these SPXs were not reported in Dzhembekova et al. (2022) as their untypical CID spectra and the lack of identification of *A. ostenfeldii* in the field samples cast doubt on the correctness of these findings. But in the light of the toxin profile of strain BS 5-D3, it becomes obvious that the original data in fact are valid and in accord with the SPX profile of strain BS 5-D3. The fact that the toxin profile of a single strain is almost identical with toxin profile of a planktonic field sample indicates a low diversity of the local *A. ostenfeldii* population, which is unusual and in contrast with other geographic regions (Tillmann et al., 2014). In a chemotaxonomic aspect of toxigenic plankton, the Black Sea seems to be a very particular environment and certainly more research including a characterization of more *A. ostenfeldii* strains is necessary.

4.3. *Yessotoxin producers*

Yessotoxins are a group of lipophilic phycotoxins regulated by the EU and are among the shellfish toxins leading to mussel farm closures in the Adriatic Sea of Italy (Riccardi et al., 2009). There also are reports of yessotoxins detected in shellfish from the Black Sea (Morton et al., 2007; Peteva et al., 2020) and these findings underscore the necessity to identify and characterize the major planktonic source species of this toxin. There are a number of YTX producing species known from the literature, including *Protoceratium reticulatum, Lingulaulax polyedra*, and a few species of *Gonyaulax* (Paz et al., 2008). All these are common members of the plankton community along the southwestern Black Sea (Dzhembekova et al., 2022), but due to lack of cultures, the actual toxin production potential of local populations of these species was not known. Based on the results presented here, we can confirm yessotoxin production for *P. reticulatum* and *L. polyedra*, whereas for one strain of *Gonyaulax* sp. and one strain of *Sourniaea diacantha* (formerly *Gonyaulax verior*) no YTX above the limit of detection could be found. Interestingly, the Black Sea strain of *Sourniaea diacantha* cluster with ribotype B, previously reported as restricted to the Pacific Ocean (Zhang et al., 2020). The large genetic distances from the other *Sourniaea diacantha* strains are consistent with earlier suggestions of cryptic diversity within this species (Zhang et al., 2020).

Yessotoxin production potential of species of *Gonyaulax* is not entirely clear. While some of the early reports on YTX in *Gonyaulax* are based on the ELISA method and thus might be questioned, more recent studies reliably detected YTX based on LC-MS/MS for *G. spinifera* (Riccardi et al., 2009), *G. lewisae* (= *G. membranaceae*) (Pitcher et al., 2019; note that the species is reported as *G. spinifera*) and *G. taylorii* (Álvarez et al., 2016). However, the taxonomy of *Gonyaulax* is challenging and what is usually reported as *G. spinifera* is now in fact known to represent one of many very similar species impossible to differentiate based on light microscopy of vegetative cells. In particular, a recent study identified the new species, *Gonyaulax montresorae* Shuning Huang, K.N. Mertens & H. Gu, as a source of yessotoxins, which in many cases likely represents the species wrongly identified as YTX-producing *G. spinifera* in other studies (Huang et al., 2025). Unfortunately, the species identity of the single strain of *Gonyaulax* isolated from the Black Sea could not be clarified, and the reason for the large sequence differences to all available *Gonyaulax* entries in Genbank remain elusive. In any case, our chemical analyses revealed that this strain does not produce yessotoxins, and the same refers to the strain of *Sourniaea diacantha*, consistent with similar findings for a strain from South Korea (Wei et al., 2020).

All six strains of *Protoceratium reticulatum* produce significant amounts of YTX and the cell quotas in the range from 1.9 to 5.4 pg $cell^{-1}$ compare well to cell quotas reported for strains of this species from other regions (Paz et al., 2007; Sala-Peréz et al., 2016). Lower levels of YTXs were detected in strains of *Lingulaulax polyedra*, where only 9 out of all 12 strains contained levels of total YTXs, most of which had levels $<$ 1pg $cell^{-1}$. Based on the cell quota and considering that in three strains of L. *polyedra* no YTX above LOD could be detected, these results show that *Protoceratium* is the major producer of YTXs in the Black Sea. However, for YTX contamination of seafood, the density of the producing species must also be considered. And here it is *Lingulaulax polyedra,* for which dense and recurrent blooms occur in the Black Sea (Terenko and Krakhmalny, 2022), so that a lower per cell production potential of this species can be counteracted by enormous bloom densities.

Furthermore, the YTX profile of the Black Sea YTX producers confirm

previous literature finding that generally *P. reticulatum* produces only YTX (Krock et al., 2008; Röder et al., 2012; Sala-Peréz et al., 2016; Wang et al., 2019) while *L. polyedra* contains other YTX variants but no YTX (Pistocchi et al., 2012; Tillmann et al., 2021). Moreover, sequence data of both species indicate that the Black Sea populations are not significantly differentiated from population from other areas of the world. The clustering of Black Sea *P. reticulatum* strains within clade B is consistent with previous investigations, which identified ribotype B as a moderate ecotype with YTX-dominated profile (Wang et al., 2019).

4.4. *Karlodinium sp. and Polykrikos hartmannii*

With respect to the diversity of HAB species in the Black Sea which are potentially ichthyotoxic or otherwise harmful to the ecosystem there is a gap of knowledge. There are only very few of such ichthyotoxic/harmful dinoflagellates in species lists for the Black Sea (Gómez and Boicenco, 2004; Moncheva and Parr, 2015; Krakhmalny et al., 2018), including *Akashiwo sanguinea, Margalefidinium polykrikoides, Karenia brevis* and *K. mikimotoi*, although the latter two species are not listed in Gómez and Boicenco (2004) and the record references provide by Krakhmalny et al. (2018) include unpublished data and unavailable grey literature only. Interestingly, not a single species of *Karlodinium* is included in all these lists. Species of *Karlodinium* are generally small and similar to many species classified as *Gymnodium* and *Gyrodinium,* and are difficult (if not impossible when using fixed samples) to be morphologically identified even at the genus level. Given the large number of small and mostly dubious *Gymnodinium* and *Gyrodinium* species entries in the Black Sea plankton reference lists, it is quite conceivable that *Karlodinium* species were previously observed but not identified as such. Indeed, more recent 18S rRNA gene metabarcoding studies have identified SSU-based OTUs suggesting the presence of the karlotoxin producing species *Karlodinium veneficum* (Dzhembekova et al., 2017b, 2022). However, there are only limited SSU rDNA sequence data available in GenBank for different *Karlodinium* species, making the molecular identification at the species level difficult. Although up to now no karlotoxins have been detected in field samples (Dzhembekova et al., 2022), including samples of the present PHYCOB 2021 cruise (Dzhembekova et al., 2025), there is a need to identify which species of *Karlodinium* are present in the Black Sea and whether they are capable of karlotoxin production. With the first laboratory strains of *Karlodinium* from this area we thus can provide first information towards this goal. With the information from the new strains, it can be recognized that an SSU-metabarcoding OTU obtained from the PHYCOB 2021 samples and identified as *Karlodinium* sp. (Dzhembekova et al., 2025) conforms with the new Black Sea strains. The sequences of both strains show that they differ significantly from other *Karlodinium* species and certainly from *K. veneficum*. However, ultrastructural studies to identify possible diagnostic morphological differences as well as potential effects of these strains of other organisms are still pending and are the subject of ongoing research. What we present here is that in both strains, none of the known karlotoxins could be detected. For *Karlodinium veneficum*, both toxic (i.e., karlotoxin-producing) and non-toxic strains have been described (Adolf et al., 2007; Place et al., 2012). Generally, it is possible that certain species or strains produce karlotoxin-like substances that are not detected by the current mass spectrometry measurement protocols. For example, while the first strain of *Karlodinium armiger* was described as producing karmitoxins (Bergholtz et al., 2005), two newly identified strains of the same species lack any of the known karmitoxins, although at least one of these new strains exhibits lytic activity and ichthyotoxicity (Pöchacker et al., 2025). With respect to lytic activity, both new Black Sea *Karlodinium* strains are non lytic, as it was the case for the strain of *Polykrikos hartmannii*. This latter species is reported from many areas of the world, sometimes occurring in bloom densities (Huang and Dong., 2001; Badylak and Phlips, 2004; Tang et al., 2013). Such blooms in an Long Island Estuary (US) were accompanied by large fish kills and *P. hartmannii* isolated from the area was experimentally shown to be ichthyotoxic (Tang et al., 2013). Although no bloom densities of *P. hartmannii* in the Black Sea have been reported so far, it is important to monitor the occurrence of this ichthyotoxic species in the Black Sea more closely. *Karlodinium* is likewise of concern: of the 17 *Karlodinium* species described so far (Guiry and Guiry, 2022), 7 are listed on the IOC reference data base of harmful algae (Lundholm et al., 2009 onwards). Therefore, more studies are needed to fully describe the diversity and toxicity of *Karlodinium* spp. in the Black Sea.

CRediT authorship contribution statement

Fuat Dursun: Writing – review & editing, Writing – original draft, Visualization, Formal analysis, Conceptualization. **Nina Dzhembekova:** Writing – review & editing, Writing – original draft, Visualization, Formal analysis, Conceptualization. **Bernd Krock:** Writing – review & editing, Formal analysis. **Jan Tebben:** Writing – review & editing, Formal analysis. **Urban Tillmann:** Writing – review & editing, Writing – original draft, Visualization, Formal analysis, Conceptualization.

Declaration of competing interest

The authors declare that they have no known competing financial interests or personal relationships that could have appeared to influence the work reported in this paper.

Acknowledgements

The authors thank Captain Tayfun Denizmen and R/V TÜBİTAK MARMARA crew for their technical support and collaboration throughout the entire cruise. We greatly acknowlede technical support of Anne Müller (DNA extraction) and Thomas Max (Toxin analyses). The study was financed by EUROFLEETS+ under SEA-Call "REGIONAL" funded from the EU H2020 Research and Innovation Programme (GA 824077). The authors acknowledge support by the Open Access Publication Funds of AWI.

Supplementary materials

Supplementary material associated with this article can be found, in the online version, at doi:10.1016/j.hal.2025.103026.

Data availability

Data will be made available on request.

References

Abdullah, N., Teng, S.T., Hanifah, A.H., Law, I.K., Tan, T.H., Krock, B., Harris, T.H., Nagai, S., Lim, P.T., Tillmann, U., Leaw, C.P., 2023. Thecal plate morphology, molecular phylogeny, and toxin analyses reveal two novel species of *Alexandrium* (Dinophyceae) and their potential for toxin production. Harmful Algae 127, 102475.

Adolf, J., Krupatkina, D., Bachvaroff, T.R., Place, A.R., 2007. Karlotoxin mediates grazing by *Oxyrrhis marina* on strains of *Karlodinium veneficum*. Harmful Algae 6, 400–412.

Álvarez, G., Uribe, E., Regueiro, J., Blanco, J., Fraga, S., 2016. Gonyaulax taylorii, a new yessotoxin-producer dinoflagellate species from Chilean waters. Harmful Algae 58, 8–15.

Aráoz, R., Ouanounou, G., Iorga, B.I., Goudet, A., Alili, D., Amar, M., Benoit, E., Molgó, J., Servent, D., 2015. The neurotoxic effect of 13,19-didesmethyl and 13-desmethyl spirolide C phycotoxins is mainly mediated by nicotinic rather than muscarinic acetylcholine receptors. Toxins 156–157.

Badylak, S., Phlips, E.J., 2004. Sppatial and temporal patterns of phytoplankton composition in a subtropical coastal lagoon, the Indian River Lagoon, Florida, USA. J. Plankton Res. 26, 1229–1247.

Bates, S.S., Hubbard, K.A., Lundholm, N., Montresor, M., Leaw, C.P., 2018. *Pseudo-nitzschia, Nitzschia,* and domoic acid: new research since 2011. Harmful Algae 79, 3–43.

Benico, G., Takahashi, K., Lum, W.M., Yniguez, A.T., Iwataki, M., 2020. The harmfull unarmoured Dinoflagellate *Karlodinium* in Japan and Philippines, with reference to ultrastructure and micropredation of *Karlodinium azanzae* sp. nov. (Kareniaceae, Dinophyceae). J. Phycol. 56, 1264–1282.

Bergholtz, T., Daugbjerg, N., Moestrup, Ø., Fernandez-Tejedor, M., 2005. On the identity of *Karlodinium veneficum* and description of *Karlodinium armiger* sp. nov. (inophyceae), based on light and electron microscopy, nuclear encoded LSU rDNA, and pigment composition. J. Phycol. 42, 170–193.
Besiktepe, S., Ryabushko, L., Ediger, D., Yilmaz, D., Zenginer, A., Ryabushko, V., Lee, R. E., 2008. Domoic acid production by *Pseudo-nitzschia calliantha* Lundholm, Moestrup et Hasle (Bacillariophyta) isolated from the Black Sea. Harmful Algae 7, 438–442.
Bodeanu, N., Roban, A., 1975. Donnés concenrnant la floraison des eaux du littoral Roumain de la mer Noire avec la péridinien *Exuviaella cordata* Ostf. Cercet. Mar. 8, 43–62.
Bodeanu, N., 2002. Algal blooms in Romanian Black Sea waters in the last two decades of the XXth century. Cercet. Mar. 34, 7–22.
Borkman, D.G., Smayda, T.J., Tomas, C.R., York, R., Strangman, W., Wright, J.L.C., 2012. Toxic *Alexandrium peruvianum* (Balech and de Mendiola) balech and Tangen in Narragansett Bay, Rhode Island (USA). Harmful Algae 19, 92–100.
Branco, S., Oliveira, M.M.M., Salgueiro, F., Vilard, M.C.P., Azevedo, S.M.F.O., Menezesa, M., 2020. Morphology and molecular phylogeny of a new PST-producing dinoflagellate species: *alexandrium fragae* sp. nov. (Gonyaulacales,dinophyceae). Harmful Algae 95, 101793.
Chomérat, N., 2016. Studies on the benthic genus *Sinophysis* (Dinophysales, Dinophyceae): I. A taxonomic investigation from Martinique Island, including two new species and elucidation of the epithecal plate pattern. Phycologia 55, 445–461.
Ciminiello, P., Fattoruso, E., Forino, M., Montresor, M., 2000. Saxitoxin and neosaxitoxin as toxic principles of *Alexandrium andersoni* (Dinophyceae) from the Gulf of Naples, Italy. Toxicon 38, 1871–1877.
Ciminiello, P., Dell'Aversano, C., Fattorusso, E., Forino, M., Grauso, L., Tartaglione, L., Guerrini, F., Pistocchi, R., 2007. Spirolide toxin profile of adriatic *Alexandrium ostenfeldii* cultures and structure elucidation of 27-hydroxy-13,19-didesmethyl spirolide C. J. Nat. Prod. 70, 1878–1883.
Clark, K., Karsch-Mizrachi, I., Lipman, D.J., Ostell, J., Sayers, E.W., 2016. GenBank. Nucl. Acids Res. 44, 67–72.
Diener, M., Erler, K., Hiller, S., Christian, B., Luckas, B., 2006. Determination of paralytic shellfish poisoning (PSP) toxins in dietary supplements by application of a new HPLC/FD method. Eur. Food Res. Technol. 224.
Dzhembekova, N., Dursun, F., Tillmann, U., Zlateva, I., Vlas, O., Slabakova, N., Möller, K., Moncheva, S., Koch, F., Boicenco, L., Aslan, E., Mutlu, S., Popov, I., Nagai, S., Krock, B., 2025. Occurrence of toxic microalgae and associated toxins in the western Black Sea: insights from the PHYCOB cruise in September 2021. Harmful Algae 151, 103025.
Dzhembekova, N., Moncheva, S., 2014. Recent trends of potentially toxic phytoplankton species along the Bulgarian Black Sea area. In: Proceedings of the Twelfth International Conference On Marine Sciences and Technologies. Varna, Bulgaria.
Dzhembekova, N., Atanasov, I., Ivanova, P., Moncheva, S., 2017a. New potentially toxic *Pseudo-nitzschia* species (Bacillariophyceae) identified by molecular approach in the Black Sea (Varna Bay). In: Proceedings of the 17th International Multidisciplinary Scientific GeoConference SGEM 2017, pp. 889–896.
Dzhembekova, N., Urusizaki, S., Moncheva, S., Ivanova, P., Nagai, S., 2017b. Applicability of massively parallel sequencing on monitoring harmful algae at Varna Bay in the Black Sea. Harmful Algae 68, 40–51.
Dzhembekova, N., Slabakova, N., Slabakova, V., Zlateva, I., Moncheva, S., 2021. Long-term trends in *pseudo-nitzschia* complex blooms in the Black Sea–is there a potential risk for ecological and human hazards. Ecol. Balk. 13, 55–75.
Dzhembekova, N., Moncheva, S., Slabakova, N., Zlateva, I., Nagai, S., Wietkamp, S., Wellkamp, M., Tillmann, U., Krock, B., 2022. New knowledge on distribution and abundance of toxic microalgal species and related toxins in the Northwestern Black Sea. Toxins 14, 685.
Farabegoli, F., Blanco, L., Rodríguez, L., Vieites, J., Cabado, A., 2018. Phycotoxins in marine shellfish: origin, occurrence and effects on humans. Mar. Drugs 16, 188.
Frangopulos, M., Guisande, C., deBlas, E., Maneiro, I., 2004. Toxin production and competitive abilities under phosphorus limitation of *Alexandrium* species. Harmful Algae 3, 131–139.
Gaillard, S., Small, H.J., Ayache, N., Tanniou, S., Hess, P., Réveillon, D., Harris, C.M., Harris, T.M., Scott, G.P., MacIntyre, A., Reece, K., 2024. Investigating the role of allelochemicals in the interaction between *Alexandrium monilatum* and other phytoplankton species. Harmful Algae 139, 102706.
Garcia-Altares, M., Casanova, A., Bane, V., Diogène, J., Furey, A., de la Iglesia, P., 2014. Confirmation of pinnatoxins and spirolides in shellfish and passive samplers from Catalonia (Spain) by liquid chromatography coupled with triple quadrupole and high-resolution hybrid tandem mass spectrometry. Mar. Drugs 12, 3706–3732.
Glibert, P.M., Anderson, D., Gentien, P., Granéli, E., Sellner, K., 2005. The global, complex phenomena of harmful algal blooms. Oceanography 18, 136–147.
Gómez, F., Boicenco, L., 2004. An annotated checklist of dinoflagellates in the Black Sea. Hydrobiologia 517, 43–59.
Guiry, M.D., Guiry, G.M., 2022. AlgaeBase. World-Wide Electronic Publication. National University of Ireland, Galway. http://www.algaebase.org. searched on 10 February 2022.
Hallegraeff, G., Enevoldsen, H., Zingone, A., 2021. Global harmful algal bloom status reporting. Harmful Algae 102, 101992.
Hallegraeff, G.M., 2010. Ocean climate change, phytoplankton community responses, and harmful algal blooms: a formidable predictive challenge. J. Phycol. 46, 220–235.
He, Z., Xu, Q., Chen, Y., Liu, S., Song, H., Wang, H., Leaw, C.P., Chen, N., 2024. Acquisition and evolution of the neurotoxin domoic acid biosynthesis gene cluster in *Pseudo-nitzschia* species. Commun. Biol. 7, 1378.
Huang, C., Dong, Q., 2001. Taxonomic and biological studies on organisms causing a large scale red tide in Zhujiang River Estuary in spring, 1998 III. Oceanol. Limnol. Sin. 32, 1–6.
Huang, S., Mertens, K.N., Derrien, A., David, O., Shin, H.H., Li, Z., Cao, X., Cabrini, M., Klisarova, D., Gu, H., 2025. *Gonyaulax montresoriae* sp. nov. (Dinophyceae) From the Adriatic Sea produces predominantly yessotoxin. Harmful Algae 141, 102761.
Kalinova, G., Mechkarova, P., Marinova, M., 2015. A study of paralytic toxins in cultured mussels from Bulgarian Black Sea. Trakia J. Sci. 13, 303–308.
Katoh, K., Rozewicki, J., Yamada, K.D., 2019. MAFFT online service: multiple sequence alignment, interactive sequence choice and visualization. Brief. Bioinform. 20, 1160–1166.
Keller, M.D., Selvin, R.C., Claus, W., Guillard, R.R.L., 1987. Media for the culture of oceanic ultraphytoplankton. J. Phycol. 23, 633–638.
Kita, T., Fukuyo, Y., 1988. Description of the gonyaulacoid dinoflagellate *Alexandrium hiranoi* sp. nov. inhabiting tidepools on Japanese Pacific coast. Bull. Plankton Soc. Jpn. 35, 1–7.
Krakhmalny, A.F., Okolodkov, J.B., Bryantseva, Y.V., Sergeeva, A.V., Velikova, V.N., Derezyuk, N.V., Terenko, G.V., Kostenko, A.G., Krakhmalny, M.A., 2018. Revision of the dinoflagellate species composition of the Black Sea. Algologia 28, 428–448.
Krakhmalnyi, A., Terenko, G., Krakhmalnyi, M., Sokolovska, O., 2024. Harmful Dinoflagelates in Odessa Bay (Black Sea). Harmful Algae News 77, 11–12.
Kremp, A., Lindholm, T., Dreßler, N., Erler, K., Gerds, G., Eirtovaara, S., Leskinen, E., 2009. Bloom forming *Alexandrium ostenfeldii* (Dinophyceae) in shallow waters of the Aland Archipelago, Northern Baltic Sea. Harmful Algae 8, 318–328.
Kremp, A., Tahvanainen, P., Litaker, W., Krock, B., Suikkanen, S., Leaw, C.P., Tomas, C., 2014. Phylogenetic relationships, morphological variation, and toxin pattern in the *Alexandrium ostenfeldii* (Dinopyhceae) complex: implications for species boundaries and identities. J. Phycol. 50, 81–100.
Kremp, A., Hansen, P.J., Tillmann, U., Savela, H., Suikkanen, S., Voß, D., Barrera, F., Jakobsen, H.H., Krock, B., 2019. Distribution of three Alexandrium species and their toxins across a salinity gradient suggest an increasing impact of GDA producing *A. pseudogonyaulax* in shallow brackish waters of Northern Europe. Harmful Algae 87, 101622.
Krock, B., Seguel, C.G., Cembella, A.D., 2007. Toxin profile of *alexandrium catenella* from the Chilean coast as determined by liquid chromatography with fluorescence detection and liquid chromatography coupled with tandem mass spectrometry. Harmful Algae 6, 734–744.
Krock, B., Alpermann, T.J., Tillmann, U., Pitcher, G.C., Cembella, A.D., 2008. Yessotoxin profiles of the marine dinoflagellates *protoceratium reticulatum* and *gonyaulax spinifera*. Ed. In: Moestrup, Ø. (Ed.), Proceedings of the 12th International Conference on Harmful Algae, Copenhagen, Denmark. ISSHA & IOC of UNNESCO, Copenhagen, pp. 303–305.
Krock, B., Busch, J.A., Tillmann, U., García-Camacho, F., Sánchez-Mirón, A., Gallardo-Rodríguez, J.J., López-Rosales, L., Andree, K.B., Fernández-Tejedor, M., Witt, M., Cembella, A.D., Place, A.R., 2017. LC-MS/MS detection of karlotoxins reveals new variants in strains of the marine dinoflagellate *Karlodinium veneficum* from the Ebro Delta (NW Mediterranean). Mar. Drugs 15, 1–20.
Krumova–Valcheva, G., Kalinova, G., 2017. *Escherichia coli* and paralytic shellfish poisoning toxins contamination of mussels farmed in Bulgarian Black Sea coast. Acta Microbiol. Bulg. 33, 30–35.
Kumar, S., Stecher, G., Li, M., Knyaz, C., 2018. Mega X: molecular Evolutionary Genetics Analysis across computing platforms. Mol. Biol. Evol. 35, 1547–1549.
Lee, K.H., Jeong, H.J., Kwon, J.E., Kang, H.C., Kim, J.H., Jang, S.H., Park, J.Y., Yoon, E. Y., Kim, J.S., 2016. Mixotrophic ability of the phototrophic dinoflagellate *Alexandrium andersonii, A. affine*, and *A. fraterculus*. Harmful Algae 59, 67–81.
Lelong, A., Hégaret, H., Soudant, P., Bates, S.S., 2012. Phycologia, 51(2), pp.168-216, 2012. *Pseudo-nitzschia* (Bacillariophyceae) species, domoic acid and amnesic shellfish poisoning: revisiting previous paradigms. Phycologia 51, 168–216.
Long, M., Krock, B., Castrec, J., Tillmann, U., 2021. Unknown extracellular and bioactive metabolites of the genus *Alexandrium*: a review of overlooked toxins. Toxins 13, 905.
Lundholm, N., Moestrup, O., Hasle, G.R., Hoef-Emden, K., 2003. A study of the *Pseudo-nitzschia pseudodelicatissima/cuspidata* complex (Bacillariophyceae): what is *P. pseudodelicatissima*? J. Phycol. 39, 797–813.
Lundholm, N., Bernard, C., Churro, C., Escalera, L., Hoppenrath, M., Iwataki, M., Larsen, J., Mertens, K., Moestrup, Ø., Murray, S., Salas, R., Tillmann, U., Zingone, A. (2009 onwards) Taxonomic reference list of harmful micro algae. accessed on 2025-02-21. 10.14284/362, Accessed at https://www.marinespecies.org/hab.
Martens, H., Tillmann, U., Harju, K., DellAversano, C., Tartaglione, L., Krock, B., 2017. Toxin variability estimations of 68 *Alexandrium ostenfeldii* (Dinophyceae) strains from The Netherlands reveal a novel abundant gymnodimine. Microorganisms 5, 29.
Martin, J.L., Haya, K., Burridge, L.E., Wildish, D.J., 1990. *Nitzschia pseudodelicatissima* - a source of domoic acid in the Bay of Fundy, eastern Canada. Mar. Ecol. Prog. Ser. 67, 117–182.
Mavrodieva, R., Moncheva, S., Hiebaum, G., 2007. Abnormal outburst of the dinoflagellate *Alexandrium ostenfeldii* (Paulsen) Balech et Tangen along the Bulgarian Black sea coast (the Bay of Sozopol) in winter–ecological surprise or ecological concern? BDUA J. Biol. II 84.
May, S.P., Burkholder, J.M., Shumway, S.E., Hégaret, H., Wikfors, G.H., 2010. Effects of the toxic dinoflagellate *Alexandrium monilatum* on survival, grazing and behavioral response of three ecologically important bivalve molluscs. Harmful Algae 9, 281–293.
Menezes, M., Branco, S., Miotto, M.C., Alves-de-Souza, C., 2018. The genus *Alexandrium* (Dinophyceae, Dinophyta) in Brazilian coastal waters. Front. Mar. Sci. 5, 421.
Mikaelyan, A.S., 1995. Winter bloom of the diatom *Nitzschia delicatula* in the open waters of the Black Sea. Mar. Ecol. Prog. Ser. 129, 241–251.

Miles, C.O., Samdal, I.A., Aasen, J.A.G., Jensen, D.J., Quilliam, M.A., Petersen, D., Briggs, L.M., Wilkins, A.L., Rise, F., Cooney, J.M., Lincoln MacKenzie, A., 2005a. Evidence for numerous analogs of yessotoxin in *Protoceratium reticulatum*. Harmful Algae 4, 1075–1091.

Miles, C.O., Wilkins, A.L., Hawkes, A.D., Selwood, A.I., Jensen, D.J., Munday, R., Cooney, J.M., Beuzenberg, V., 2005b. Polyhydroxylated amide analogs of yessotoxin from *Protoceratium reticulatum*. Toxicon 45, 61–71.

Möller, K., Tillmann, U., Pöchhaker, M., Varga, E., Krock, B., Koch, F., Harris, T.M., Meunier, C., 2024. Toxic effects of an emerging HAB species *Alexandrium pseudogonyaulax* (Dinophyceae) on selected species of the marine food chain. Harmful Algae 138, 102705.

Moncheva, S., Petrova-Karadjova, V., Palazov, A., 1995. Harmful algal blooms along the Bulgarian Black Sea Coast and possible paterns of fish and zoobenthic mortalities. In: Lassus, P., Arzul, G., Gentien, P., Marcaillou, C. (Eds.), Harmful Marine Algal Blooms. Lavoisier Publ. Inc, pp. 193–298.

Moncheva, S., Gotsis-Skretas, O., Pagou, K., Krastev, A., 2001. Phytoplankton blooms in Black Sea and Mediterranean coastal ecosystems subjected to anthropogenic eutrophication: similarities and differences. Estuar. Coast. Shelf Sci. 53, 281–295.

Moncheva, S., Parr, B., 2015. Black Sea Monitoring Guidelines-Phytoplankton. Black Sea Commission, Istanbul Turkey.

Moncheva, S., Boicenco, L., Mikaelyan, A., Zotov, A., Dereziuk, N., Gvarishvili, C., Slabakova, N., Mavrodieva, R., Vlas, O., Pautova, L., 2019. 1.3.2 Phytoplankton. In: Krutov, A. (Ed.), State of the Environment of the Black Sea (2009-2014/5). Publications of the Commission on the Protection of the Black Sea Against Pollution (BSC, Istanbul, Turkey, pp. 225–285.

Montresor, M., Marino, D., Zingone, A., Dafnis, G., 1990. Three *Alexandrium* species from coastal thyrrhenian waters (mediterranean Sea). In: Granéli, E., Sundström, B., Edler, L., Anderson, D.M. (Eds.), Toxic Marine Phytoplankton. Elsevier, New York, pp. 82–87.

Montresor, M., John, U., Beran, A., Medlin, L.K., 2004. *Alexandrium tamutum* sp. nov. (Dinophyceae): a new nontoxic species in the genus *Alexandrium*. J. Phycol. 40, 398–411.

Morton, S.L., Vershinin, A., Leighfield, T., Smith, L., Quilliam, M., 2007. Identification of yessotoxin in mussels from the Caucasian Black Sea Coast of the Russian Federation. Toxicon 50, 581–584.

Morton, S.L., Vershinin, A., Smith, L.L., Leighfield, T.A., Pankov, S., Quilliam, M.A., 2009. Seasonality of *dinophysis* spp. And *prorocentrum lima* in Black Sea phytoplankton and associated shellfish toxicity. Harmful Algae 8, 629–636.

Nesterova, D., Moncheva, S., Mikaelyan, A., Vershinin, A., Akatov, V., Boicenco, L., Aktan, Y., Sahin, F., Gvarishvili, T., 2008. Chapter 5. The state of phytoplankton. In: Oguz, T. (Ed.), State of the Environment of the Black Sea (2001–2006/7). Black Sea Commission Publications, Istanbul, Turkey, pp. 133–167, 2008-3.

Nieva, J.A., Krock, B., Tillmann, U., Tebben, J., Zurhelle, C., Bickmeyer, U., 2020a. Gymnodimine A and 13-desMethyl spirolide C alter intracellular calcium levels via acetylcholine receptors. Toxins 12, 751.

Nieva, J.A., Tebben, J., Tillmann, U., Wohlrab, S., Krock, B., 2020b. Mass spectrometry-based characterization of new spirolides from *Alexandrium ostenfeldii* (Dinophyceae). Mar. Drugs 18, 505.

Nunn, G.B., Theisen, B.F., Christensen, B., Arctander, P., 1996. Simplicity-correlated size growth of the nuclear 28S ribosomal RNA D3 expansion segment in the crustacean order Isopoda. J. Mol. Evol. 42, 211–223.

Orr, R.J.S., Stuken, A., Rundberget, T., Eikrem, W., Jakobsen, K.S., 2011. Improved phylogenetic resolution of toxic and non-toxic *Alexandrium* strains using a concatenated rDNA approach. Harmful Algae 10, 676–688.

Paz, B., Riobó, P., Ramilo, I., Franco, J.M., 2007. Yessotoxins profile in strains of *Protoceratium reticulatum* from Spain and USA. Toxicon 50, 1–17.

Paz, B., Daranas, A.H., Norte, M., Riobó, P., Franco, J.M., Fernández, J.J., 2008. Yessotoxins, a group of marine polyether toxins: an overview. Mar. Drugs 6, 73–102.

Peneva, V., Gogov, Y., Kalinova, G., Slavova, A., 2011. Application of HPLC method for determination of ASP toxins in bivalve molluscs. In: The Jubilee Scientific Session –110 years National Diagnostic Science-and-Research Veterinary Medical Institute‖ Sofia, 08 - 09.11. pp 210–213.

Peteva, Z., Krock, B., Georgieva, S., Gerasimova, A., Stancheva, M., Makedonski, L., 2018. Summer profile of lipophilic toxins in shellfish from the Black Sea, Bulgaria. Ovidius Univ. Ann. Chem. 29, 117–121.

Peteva, Z.V., Kalinova, G.N., Krock, B., Stancheva, M.D., Georgieva, S.K., 2019. Evaluation of paralytic shellfish poisoning toxin profile of mussels from Bulgarian North Black Sea coast by HPLC-FlD with post and pre-column derivatization. Bulg. Chem. Commun. 51, 233–240.

Peteva, Z.V., Krock, B., Stancheva, M.D., Georgieva, S.K., 2020. Comparison of seasonal and spatial phycotoxin profiles of mussels from South Bulgarian coast. Bulg. Chem. Commun. 52, 16–21.

Pistocchi, R., Guerrini, F., Pezzolesi, L., Riccardi, M., Vanucci, S., Ciminiello, P., Dell'Aversano, C., Forino, M., Fattorusso, E., Tartaglione, L., Milandri, A., Pompei, M., Cangini, M., Pigozzi, S., Riccardi, E., 2012. Toxin levels and profiles in microalgae from the North-Western Adriatic sea-15 years of studies on cultured species. Mar. Drugs 10, 140–162.

Pitcher, G.C., Foord, C.J., Macey, B.M., Mansfield, L., Mouton, A., Smith, M.E., Osmond, S.J., van der Molen, L., 2019. Devastating farmed abalone mortalities attributed to yessotoxin-producing dinoflagellates. Harmful Algae 81, 30–41.

Place, A.R., Bowers, H.A., Bachvaroff, T.R., Adolf, J., 2012. Karlodinium veneficum - the little dinoflagellate with a big bite. Harmful Algae 14, 179–195.

Pöchacker, M., Tillmann, U., Marko, D., Varga, E., 2025. Intraspecific variabilty within *Karlodinium armiger* (Dinophyceae) on a toxicological and metabolomic level. Harmful Algae 143, 102808.

Riccardi, M., Guerrini, F., Roncarati, F., Milandri, A., Cangini, M., Pigozzi, S., Riccardi, E., Ceredi, A., Ciminiello, P., Dell'Aversano, C., Fattorusso, E., Forino, M., Tartaglione, L., Pistocchi, R., 2009. *Gonyaulax spinifera* from the Adriatic sea: toxin production and phylogenetic analysis. Harmful Algae 8, 279–290.

Röder, K., Hantzsche, F.M., Gebühr, C., Miene, C., Helbig, T., Krock, B., Hoppenrath, M., Luckas, B., Gerdts, G., 2012. Effects of salinity, temperature and nutrients on growth, cellular characteristics and yessotoxin production of *Protoceratium reticulatum*. Harmful Algae 15, 59–70.

Ronquist, F., Huelsenbeck, J.P., 2003. MrBayes 3: bayesian phylogenetic inderence under mixed models. Bioinformatics 19, 1572–1574.

Ryabushko, L.I., 2003a. Atlas of Toxic Microalgae of the Black Sea and the Sea of Azov. Ministry of Defence of Ukraine, National Academy of Sciences of Ukraine, Scientific Center of Armed Forces of Ukraine, Sevastopol, Ukraine.

Ryabushko, L.I., 2003b. Potentially Harmful Microalgae of the Azov and Black Sea Basin. Institute of Biology of the Southern Seas, National Academy of Sciences of the Ukraine, Sevastopol: ECOSI-Gidrofizica.

Sala-Peréz, M., Alpermann, T.J., Krock, B., Tillmann, U., 2016. Growth and bioactive secondary metabolites of arctic *Protoceratium reticulatum* (Dinophyceae). Harmful Algae 55, 85–96.

Salgado, P., Riobó, P., Rodríguez, F., Franco, J.M., Bravo, I., 2015. Differences in the toxin profiles of *Alexandrium ostenfeldii* (Dinophyceae) strains isolated from different geographic origins: evidence of paralytic toxin, spirolide, and gymnodimine. Toxicon 103, 85–98.

Sampedro, N., Franco, J.M., Zapata, M., Riobóo, P., Garcés, E., Penna, A., Caillaud, A., Diogéne, J., Cacho, E., Camp, J., 2013. The toxicity and intraspecific variability of *alexandrium andersonii* Balech. Harmful Algae 25, 26–38.

Sansone, C., Nuzzo, G., Galasso, C., Casotti, R., Fontana, A., Romano, G., Ianora, A., 2018. The marine dinoflagellate *Alexandrium andersoni* induces cell death in lung and colorectal tumor cell lines. Mar. Biotechnol. 20, 343–352.

Sato, S., Nishimura, T., Uehara, K., Sakanari, H., Tawong, W., Hariganeya, N., Smith, K., Rhodes, L., Yasumoto, T., Taira, Y., Suda, S., 2011. Phylogeography of *Ostreopsis* along west Pacific coast, with special reference to a novel clade from Japan. PLoS ONE 6 e27983.

Scholin, C.A., Herzog, M., Sogin, M., Anderson, D.M., 1994. Identification of group- and strain-specific genetic markers for globally distributed *Alexandrium* (Dinophyceae). II. Sequence analysis of a fragment of the LSU rRNA gene. J. Phycol. 30, 999–1011.

Sleno, L., Windust, A.J., Volmer, D.A., 2004. Structural study of spirolide marine toxins by mass spectrometry. Part I: fragmentation pathways of 13-desmethyl spirolide C by collision-induced dissociation and infrared multiphon dissociation mass spectrometry. Anal. Bioanal. Chem. 378, 969–976.

Stüken, A., Orr, R.J.S., Kellmann, R., Murray, S.A., Neilan, B.A., Jakobsen, K.S., 2011. Discovery of nuclear-encoded genes for the neurotoxin saxitoxin in dinoflagellates. PLoS ONE 6 e20096.

Tang, Y.Z., Harke, M., Gobler, C.J., 2013. Morphology, phylogeny, dynamics, and ichtyotoxicity of Phaeopolykrikos hartmanii (Dinophyceae) isolatates and blooms from New York, USA. J. Phycol. 49, 1084–1094.

Terao, K., Ito, E., Murakami, M., Yamaguchi, K., 1989. Histopathological studies on experimental marine toxin poisoning—III. Morphological changes in the liver and Thymus of male ICR mice induced by Goniodomin A, isolated from the dinoflagellate *goniodoma pseudogoniaulax*. Toxicon 27, 269–271.

Terenko, G., Krakhmalny, A., 2022. Red tide of *lingulodinium polyedrum* (Dinophyceae) in Odesa Bay (Black Sea). Turk. J. Fish. Aquat. Sci. 22. TRJFAS20312.

Terenko, L., Terenko, G., 2012. Dominant *Pseudo-nitzschia* (Bacillariophyta) species in the Black Sea (Ukraine). Bot. Lith. 18, 27–34.

Thompson, J.D., Higgins, D.G., Gibson, T.J., 1994. CLUSTAL W: improving the sensitivity of progressive multiple sequence alignment through sequence weighting, position-specific gap penalties and weight matrix choice. Nucl. Acids Res. 22, 4673–4680.

Tillmann, U., Kremp, A., Tahvanainen, P., Krock, B., 2014. Charaterization of spirolid producing *Alexandrium ostenfeldii* (Dinophyceae) from the western Arctic. Harmful Algae 39, 259–270.

Tillmann, U., Bantle, A., Krock, B., Elbrächter, M., Gottschling, M., 2021. Recommendations for epitypification of dinophytes exemplified by *Lingulodinium polyedra* and molecular phylogenetics of the Gonyaulacales based on curated rRNA sequence data. Harmful Algae 104, 101956.

Tillmann, U., Dzhembekova, N., Vlas, O., Krock, B., Boicenco, L., Dursun, F., 2025. Diversity of Amphidomataceae (Dinophyceae) in the Black Sea, including description of *Amphidoma pontica* sp. nov. Phycol. Res. in press.

Touzet, N., Franco, J.M., Raine, R., 2007. Characterization of nontoxic and toxin-producing strains of *Alexandrium minutum* (Dinophyceae) in Irish coastal waters. Appl. Environ. Microbiol. 73, 3333–3342.

Türkoğlu, M., Koray, T., 2002. Phytoplankton species' succession and nutrients in the southern Black Sea (Bay of Sinop). Turk. J. Bot. 26, 235–252.

Van de Waal, D.B., Tillmann, U., Martens, H., Krock, B., van Scheppingen, Y., John, U., 2015. Characterization of multiple isolates from an *alexandrium ostenfeldii* bloom in The Netherlands. Harmful Algae 49, 94–104.

Velikova, V., Moncheva, S., Petrova, D., 1999. Phytoplankton dynamics and red tides (1987–1997) in the Bulgarian Black Sea. Water Sci. Technol. 39, 27–36.

Vershinin, A., Kamnev, A., 2001. Harmful algae in Russian European coastal waters. Harmful Algae Blooms 112–115, 2000.

Vershinin, A.O., Moruchkov, A.A., Leighfield, T., Sukhanova, I.N., Pankov, S.L., Morton, S.L., Ramsdell, J.S., 2005. Potentially toxic algae in Northeast Black Sea coastal phytoplankton in 2000-2002. Oceanology 45, 240–248.

Vershinin, A.O., Morton, S., Leighfield, T., Pankov, S., Quilliam, M., Ramsdell, J.S., 2006. *Alexandrium* in the Black Sea - identity, ecology and PSP toxicity. Afr. J. Mar. Sci. 28, 209–213.

Vershinin, A.O., Velikova, V.N., 2008. New records and commonly misidentified dinoflagellates from the Black Sea. In: Proceedings of the Modern Problems of Algology: Abstracts of the International Scientific Conference and the VII Workshop on Marine Biology, pp. 416–430, 9–13 June 2008. Rostov-on-Don.

Wang, N., Mertens, K.N., Krock, B., Luo, Z., Derrien, A., Pospelova, V., Liang, Y., Billien, G., Smith, K., Wietkamp, S., Tillmann, U., Gu, H., 2019. Pseudocryptic speciation in *Protoceratium reticulatum*. Harmful Algae 88, 101610.

Weber, C., Olesen, A.K.J., Krock, B., Lundholm, N., 2021. Salinity, a climate-change factor affecting growth, domoic acid and isodomoic acid C content in the diatom *pseudo-nitzschia seriata* (Bacillariophyceae). Phycologia 60, 619–630.

Wei, Z., Zhun, L., Mertens, K., Derrien, A., Pospelova, N., Carbonell-Moore, C., Bagheri, S., Matsuoka, K., Sin, H.H., Gu, H., 2020. Reclassification of *Gonyaulax verior* (Gonyaulacales, Dinophyceae) as *Sourniaea diacantha* gen. et comb. nov. Phycologia 59, 246–260.

White, T.J., Bruns, T., Lee, S., Taylor, J.D., 1990. Amplification and direct sequencing of fungal ribosomal RNA genes for phylogenetics. In: Innis, M.A., Gelfand, D.H., Sninsky, J.J., White, T.J. (Eds.), PCR Protocols: A Guide to Methods and Applications. Academic Press, San Diego, pp. 315–322.

Zaitsev, Y., Mamaev, V., 1997. Biological Diversity in the Black Sea: A Study of Change and Decline. United Nations Publishing, New York, NY, USA.

Zhang, W., Mertens, K.N., Derrien, A., Pospelova, V., Carbonell-Moore, M.C., Bagheri, S., Matsuoka, K., Shin, H.H., Gu, H., 2020. Reclassification of Gonyaulax verior (Gonyaulacales, Dinophyceae) as *Sourniaea diacantha* gen. et comb. nov. Phycologia 59 (3), 246–260.

Zmerli Triki, H., Daly-Yahia, O.K., Malouche, D., Komiha, Y., Deidun, A., Brahim, M., Laabir, M., 2014. Distribution of resting cysts of the potentially toxic dinoflagellate *Alexandrium pseudogonyaulax* in recently-deposited sediment within Bizerte Lagoon (Mediterranean coast, Tunisia). Mar. Pollut. Bull. 84, 172–181.